Attributes of Bi-Directional Turbomachinery for Pumped Thermal Energy Storage

by

Joseph Donald Chiapperi

B.S., Clarkson University (Honors) (2019)

Submitted to the Department of Aeronautics and Astronautics
in partial fulfillment of the requirements for the degree of

Master of Science in Aeronautics and Astronautics

at the

MASSACHUSETTS INSTITUTE OF TECHNOLOGY

June 2021

Author .....
Department of Aeronautics and Astronautics
May 18, 2021

Certified by .....
Choon Sooi Tan
Senior Research Engineer
Thesis Supervisor

Certified by .....
Edward M. Greitzer
H. N. Slater Professor of Aeronautics and Astronautics
Thesis Supervisor

Accepted by .....
Zoltan S. Spakovszky
Professor, Aeronautics and Astronautics
Chair, Graduate Program Committee

Attributes of Bi-Directional Turbomachinery for Pumped Thermal Energy Storage

by

Joseph Donald Chiapperi

Submitted to the Department of Aeronautics and Astronautics
on May 18, 2021, in partial fulfillment of the
requirements for the degree of
Master of Science in Aeronautics and Astronautics

Abstract

In this thesis we (i) present a methodology for determining the aerodynamic performance of bi-directional turbomachines for pumped thermal energy storage, i.e., turbomachines designed to operate with both forward and backward flow, (ii) carry out performance computations for such turbomachines, and (iii) propose principles for conceptual design of these devices. Focus is placed on using the energy storage cycle not to only identify the unique requirements placed on bi-directional turbomachines, but also to estimate what effect these requirements have on the round-trip efficiency of the energy storage process. In particular, it is shown how the difference between aerodynamic loading in forward and in backward operation causes the blading to work at incidences leading to performance below the blading's maximum efficiency.

The proposed design principles use a 50MW counter-rotating bi-directional turbomachine, being developed by Brayton Energy LLC, as a context from which to assess different features. The description of the design principles includes determination of the appropriate number of stages, definition of relevant non-dimensional parameters for blading selection, and optimization of two-dimensional blading for bi-directional operation. The assessment of stage count shows the relationship between relative Mach number, pressure ratio, and round-trip efficiency. The non-dimensional parameter assessment creates a bi-directional analogue to existing "Smith charts", for single direction turbomachines, using camber and stagger. The two-dimensional blade shape evaluation and optimization shows how the blade profile can be modified to address the unique requirements of a bi-directional turbomachine, enabling an increase in round-trip efficiency of 2 percentage points compared to a baseline configuration.

Thesis Supervisor: Choon Sooi Tan
Title: Senior Research Engineer

Thesis Supervisor: Edward M. Greitzer
Title: H. N. Slater Professor of Aeronautics and Astronautics

Acknowledgments

I would first like to thank my advisors, Dr. Tan and Professor Greitzer, whose knowledge and support were indispensable to me. I am grateful not only for the research guidance, but for helping me to stay on track through the Covid-19 pandemic. I would also like to thank Prof. Drela and Prof. Cumpsty for insightful discussions and advice.

I am grateful to the team at Brayton Energy in Hampton, NH; Jim Kesseli, Paul Harris, and Tom Wolf, for the helpful discussions and direction. I would also like to thank the team at the Department of Energy ARPA-e; Scott Litzelman, Vivien Lecoustre, and Max Tuttman, and the DAYS program which funded this research.

I want to acknowledge the amazing support of the MIT Gas Turbine Lab. Both in-person and online, it was the students, staff, and faculty of the GTL who always made me feel like a part of a community. In particular, I'd like to show my deepest appreciation for the GTL sysadmins, who made sure we could keep working from home as the institute rapidly shifted to online learning.

Last, but certainly not least, I want to thank my friends and family for endlessly supporting me throughout this experience. To Aaron, Abbi, Brittney, Collin, and Marissa; y'all are amazing and keep me sane. I would have never been able to write a thesis during a pandemic without our virtual gatherings. Thank you Mom, Dad, Nat, Daisy, and Lydia for the love, support, and guidance. You kept me grounded through these strange years.

THIS PAGE INTENTIONALLY LEFT BLANK

Contents

List of Figures

Chapter 1

Introduction

1.1 Pumped Thermal Energy Storage

Renewable energy sources have a common drawback which hampers their widespread application, namely that the rate at which they produce electricity is not aligned with the rate at which energy is consumed. For example, wind and solar farms are dependent on the weather to produce electricity and therefore must be supplemented with a more controllable source of energy to reliably supply an electric grid [2][12]. A large-scale energy storage device is thus necessary to make renewable energy sources a feasible replacement for fossil fuels.

Pumped Thermal Energy Storage (PTES) provides a possible technology to fill this role. A PTES system stores electrical energy in the form of a thermal potential. A heat pump is used to create this thermal potential, moving heat from a cold reservoir to a hot reservoir. When the energy is to be returned, this thermal potential is used to produce electricity by driving a heat engine.

For the PTES system described here, both of these modes operate with a Brayton cycle. Figure 1-1 shows a schematic for such a system. Here, the green path indicates the heat engine and the orange path indicates the heat pump, with the wide arrows denoting heat exchange. The hot and cold reservoirs are denoted by the red and blue areas, respectively, interfacing with the working fluid through heat exchangers. This type of technology was evaluated by Laughlin [12] and examined in further detail by

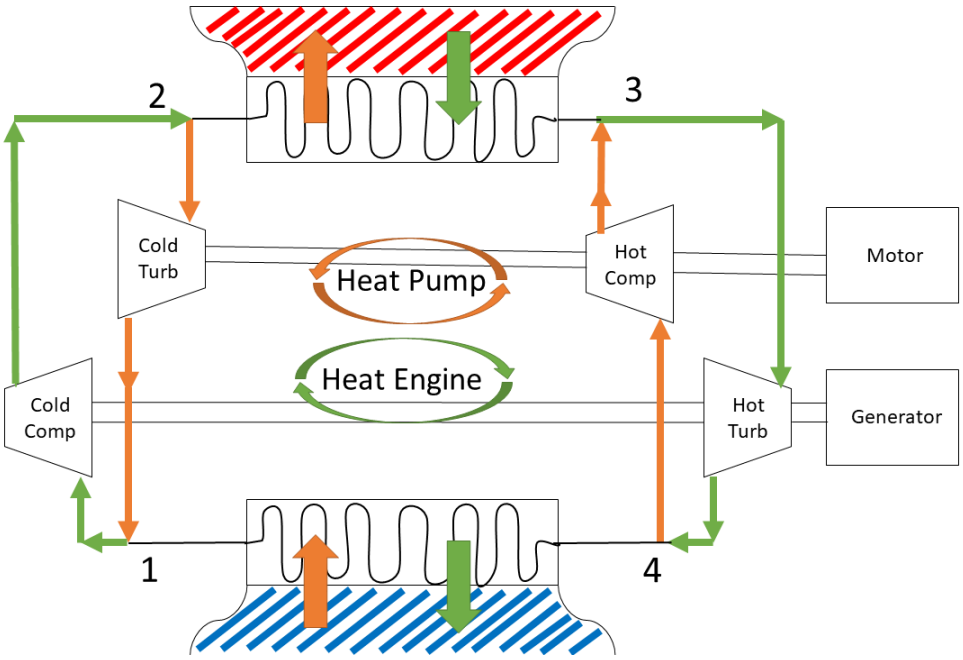

Figure 1-1: Pumped-Thermal Energy Storage System Schematic

Brayton Energy LLC in conjunction with Google [9].

The systems which have been developed all employ separate components for the energy storage and for the energy withdrawal processes. A set of turbomachinery runs as a heat pump while another set is idle. Then, when the energy is to be withdrawn, the idle turbomachinery is used in the heat engine, while the heat pump becomes idle. Whatever the state of the PTES system, half of the turbomachinery is always sitting idle, because of the single-direction nature of the compressors and turbines in the system. If a bi-directional turbomachine could be built to operate as a compressor in one direction and a turbine in the other however, there would be no components sitting idle, and the system would be potentially cheaper and less complex. Figure 1-2 shows a schematic of a PTES system with bi-directional turbomachines. The design of such turbomachines is the focus of this thesis.

1.2 Ideal Cycle Analysis of PTES System

The ideal cycles for the systems in Figures 1-1 and 1-2 are identical, and they are shown in the T-S diagram in Figure 1-3. For a bi-directional system the same tur-

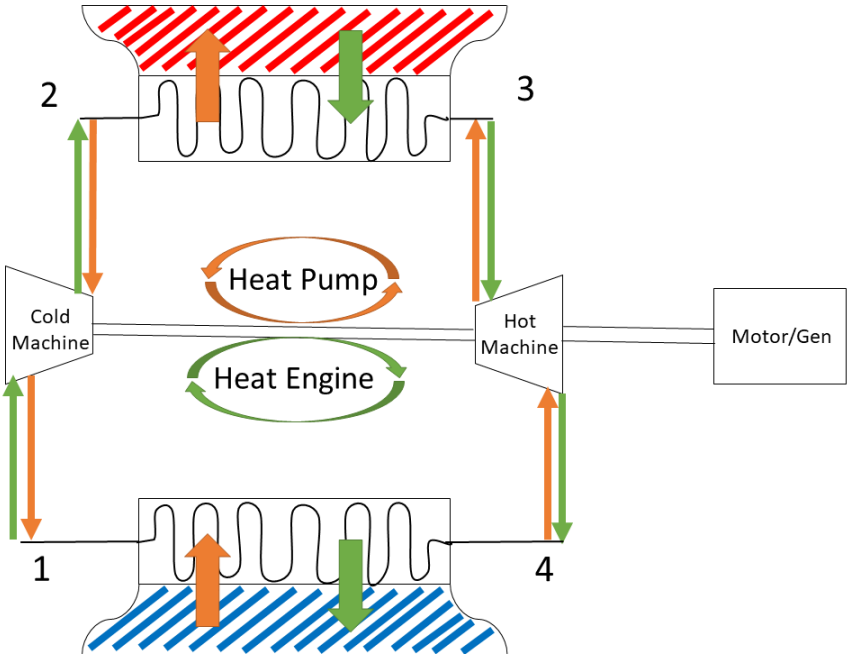

Figure 1-2: PTES System with Bi-Directional Turbomachines

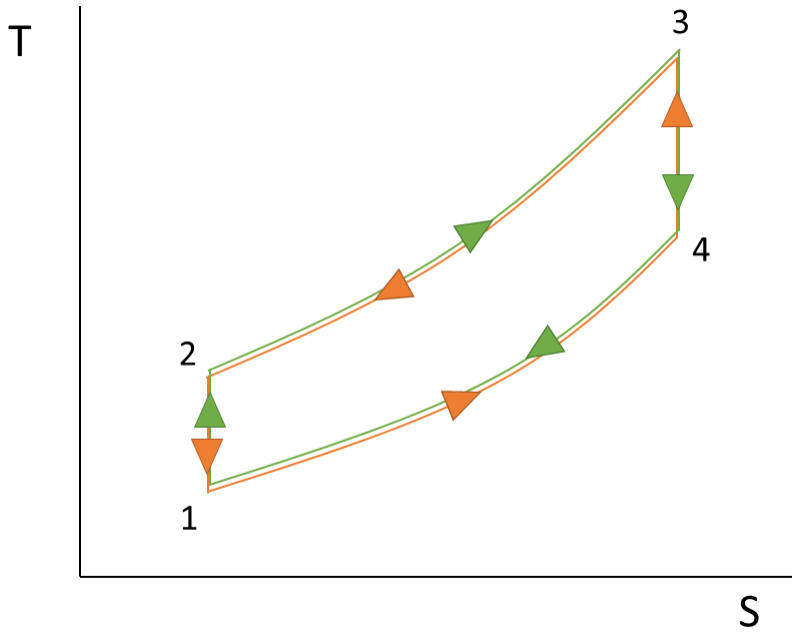

Figure 1-3: Ideal Thermal Storage Cycle T-S Diagram

bomachine is used as the turbine of the heat pump and the compressor of the heat engine, and it is referred to as the "cold machine", which operates between points 1 and 2 on the cycle. A single turbomachine is also used as the compressor of the heat pump and the turbine of the heat engine, referred to as the "hot machine", which operates between points 3 and 4.

The schematics in Figures 1-1 and 1-2 show simplified hot and cold reservoirs. To have reversible heat addition processes, the system uses multiple storage tanks and a reverse flow heat exchanger. A regenerator is also used to increase the temperature difference between the hot and cold reservoirs. The regenerator is a heat exchanger which transfers heat between points 2 and 4 in Figure 1-2.

A more complete schematic with the 2 reservoir heat exchangers and the regenerator is shown in Figure 1-4 and the corresponding T-S diagram is shown in Figure 1-5. The stations in this schematic and T-S diagram are renumbered to include the regenerator. The hot and cold reservoirs are shown here as two separate tanks connected by a reverse flow heat exchanger. In the heat pump, when the working fluid moves from station 4 to 3, depositing heat into the hot reservoir, the hot storage fluid moves from 3 to 4 and its temperature increases from T_H^- to T_H^+. In the heat engine, the opposite occurs. The working fluid moves from 3 to 4 and is heated, while the hot storage fluid moves from 4 to 3 and is cooled from T_H^+ to T_H^-. The same concepts apply to the cold reservoir, where the two tanks have temperatures of T_C^- and T_C^+. The regenerator transfers heat between the two sides of the system and acts between stations 2 and 3, and stations 5 and 6. The T-S diagram in Figure 1-5 show these heat transfers as wide green and orange arrows. The green and orange triangles indicate the direction in which the working fluid flows for each mode of operation.

The cycles in both modes of operation are defined by 2 parameters: the pressure ratio and the normalized temperature difference between hot storage and ambient temperatures, as in Equation 1.1.

$$Normalized\,Temperature\,Difference = \frac{T_H^+ - T_{amb}}{T_{amb}} \tag{1.1}$$

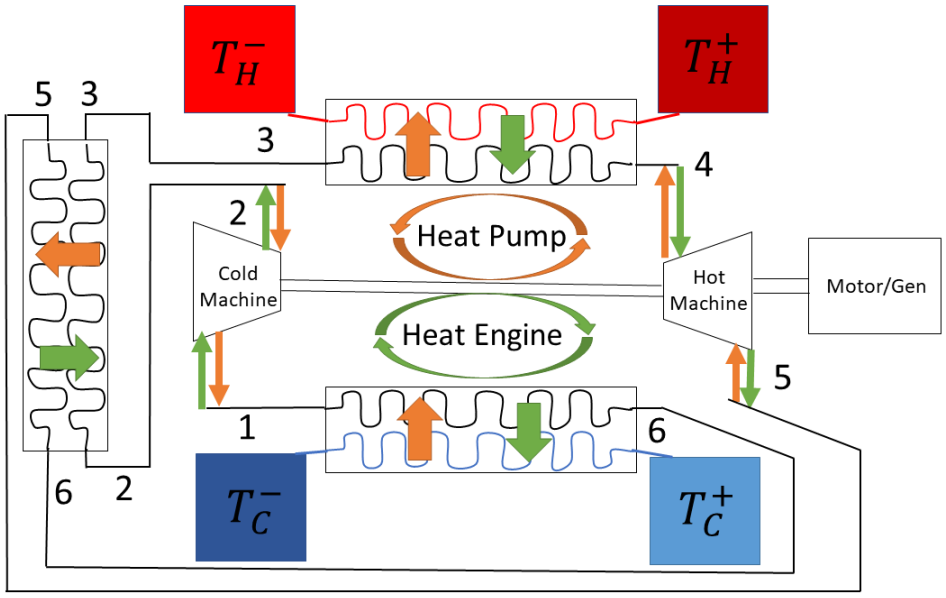

Figure 1-4: PTES System with Bi-Directional Turbomachines, Regenerator, Storage Tanks, and Reverse Flow Heat Exchangers

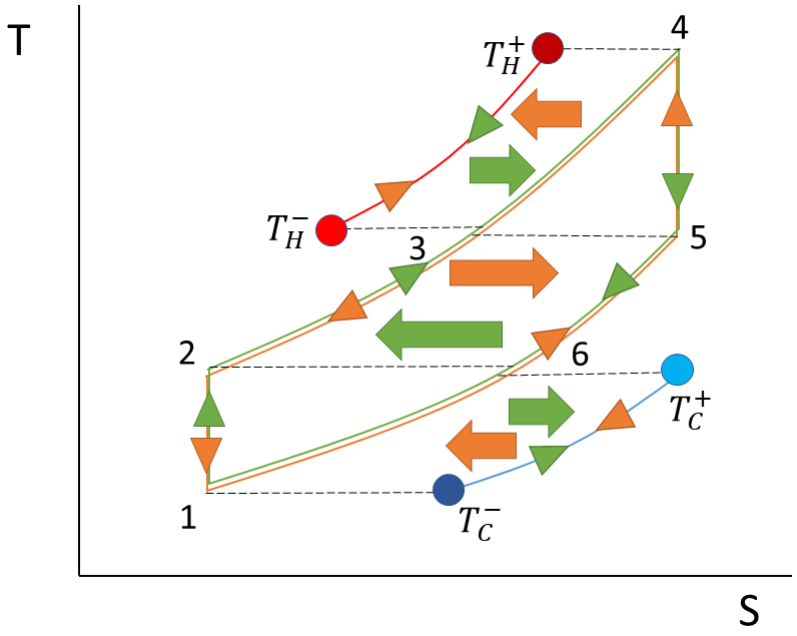

Figure 1-5: Ideal Thermal Storage Cycle T-S Diagram, Including Storage Heat Exchangers and Regenerator

In the ideal cycle, the ambient temperature is equal to T_C^+. On the T-S diagram, the pressure ratio sets how wide the cycle is, and the temperature difference sets how tall the cycle is. The main design parameter for the turbomachines in a PTES cycle is the pressure ratio.

The primary performance metric for an energy storage device is the round-trip efficiency (RTE), defined as the ratio between energy stored and energy withdrawn, as in Equation 1.2.

$$RTE = \frac{E_{out}}{E_{in}} \tag{1.2}$$

If 10 MWh of electricity were used to drive the heat pump, and then 10 MWh were later produced by the heat engine, the RTE would be unity. If some stored energy were lost as waste heat, RTE would be less than unity. The T-S diagrams in Figures 1-3 and 1-4 show the ideal PTES cycle, with reversible heat transfers and isentropic turbomachines. For a reversible cycle, the RTE is unity, no matter the pressure ratio of the turbomachines or the temperatures of the storage tanks. With irreversibility however, the RTE falls below unity, as we will see in section 2.1.2

1.3 Motivation for Bi-Directional Turbomachines

There are three main motivations for using bi-directional turbomachines in an energy storage system. First, is a potential cost advantage. Instead of requiring 4 single direction turbomachines, the system would require 2 bi-directional turbomachines. Second, the ducting network of the storage system becomes simpler. With single direction turbomachines, large valves and ducting are needed to direct the working fluid to the appropriate turbomachine. With bi-directional turbomachines, the gas path is now one single circuit and these valves are not necessary. Third, there is no warm-up period when changing modes. With single direction turbomachines, one compressor and one turbine are always sitting idle and at ambient temperature. When changing from storage to generation, or vice versa, these turbomachines need to come to operational temperature. With bi-directional turbomachines, the system components are always in use and at the correct temperature. On the debit side, it

may be expected that using bi-directional turbomachines instead of single direction turbomachines may negatively impact the round-trip efficiency. In the case of energy storage however, cost can be more important than efficiency; "storage of electricity is fundamentally about value, not about conserving energy." [Laughlin, 12]

1.4 Thesis Scope

This thesis first discusses the details of the PTES cycle. Irreversibilities are added to to the ideal cycle to produce a real PTES cycle and to understand the relationship between turbomachine efficiency and round-trip efficiency. The real cycle also shows how the turbomachine requirements change with turbomachine efficiency.

Using the requirements identified by the real cycle analysis, several design guidelines are developed to maximize RTE. These guidelines are developed using Brayton Energy LLC's 50MW bi-directional turbomachine architecture as a framework from which to assess different features. The 50MW architecture is a counter-rotating turbomachine with no stators between the rotors. As such, some design features (such as variable stators) are not considered in this thesis. The design features discussed in this thesis are assessed using 2D CFD (MISES [7]), 2D blade optimization tools (MILOP [5]), and a model of the PTES cycle.

1.5 Contributions

There are three main contributions of this thesis. First, several unique requirements of bi-directional turbomachines are identified. In addition to the requirement of efficiency for flow in two directions, analysis of the real storage cycle shows that the cold machine has different aerodynamic loading for each direction. Further, this *non-symmetric*[1] loading means there can be repeating stages in only one direction.

Second, the impact of these unique requirements on RTE is assessed. It is shown that non-symmetric loading requirement means that a bi-directional turbomachine

[1]The term, "non-symmetric" is used here to describe a behavior which is different for operation in one direction than in the other

cannot operate at its own maximum efficiency in both directions, reducing RTE compared to what might be achieved with single-direction turbomachines.

Third, several design guidelines for bi-directional turbomachines are identified. These guidelines fall into 3 categories; stage count, non-dimensional parameters, and detailed 2D blade shapes. The assessment of stage count shows the relationship between relative Mach number, pressure ratio, and round-trip efficiency. The non-dimensional parameter assessment creates a bi-directional analogue to existing "Smith charts" for compressors [3], using camber and stagger. The detailed 2D blade shape assessment shows how the blade profile can be shaped to address the unique requirements for a bi-directional turbomachine.

Chapter 2

Real Cycle Definition and Details

The first step in developing a bi-directional turbomachine is to define the environment in which such a turbomachine will operate. This includes defining the Pumped Thermal Energy Storage cycle, and identifying the impact that the turbomachinery will have on it. In this chapter, we describe the thermodynamic cycle of a PTES system and discuss the sensitivity of the cycle to the performance of the components.

2.1 Cycle Definition for PTES Systems

PTES systems operate in two modes: generation and charge. In the generation mode, energy is withdrawn from the thermal storage and fed into the electric grid. This mode is a Brayton cycle heat engine that operates between hot and cold storage tanks. In the charge mode, energy from the grid is used to run the system as a heat pump, moving heat from the cold tanks to the hot tanks, operating on a reverse Brayton cycle. In this section, we expand from the ideal (reversible) PTES cycle discussed in the introduction to describe the real PTES cycle and Round-Trip Efficiency (RTE), which is the primary performance metric for a PTES system.

2.1.1 Round-Trip Efficiency

The primary performance metric for PTES systems is the Round-Trip Efficiency (RTE). This is a ratio of how much energy can be withdrawn from the system to the amount of energy originally deposited, defined in Equation 1.2, and repeated here in Equation 2.1.

$$RTE = \frac{E_{out}}{E_{in}} \tag{2.1}$$

In the ideal cycle shown in Figure 1-5, RTE is equal to 1. As irreversibilities are added to the cycle, some of the stored energy will be rejected to the environment as waste heat. Equation 2.2 incorporates this into an alternate definition for RTE.

$$RTE = 1 - \frac{Q_{rej}}{E_{in}} \tag{2.2}$$

The rejected heat, $Qrej$, increases as irreversibilities increase, meaning that RTE is less than unity for real cycles.

2.1.2 Real PTES Cycle

Figure 2-1 shows the T-S diagram for a real thermal storage cycle. There are differences from the ideal cycle in Figure 1-5.

The first difference from the ideal cycle is the addition of losses in the turbomachines. In the ideal cycle the turbomachines are treated as isentropic, so the adiabatic compression and expansion are vertical lines in the T-S diagram. For a real cycle, the irreversibilities produce tilted lines on the T-S diagram. The second difference in the real cycle is nonzero approach temperatures for the heat exchangers. An ideal heat exchanger would not have heat transfer across a finite temperature difference, and both fluids would be the same temperature as each other through the heat exchanger. For example, the temperature at location 1 would be the same as T_C^- and the temperature at location 6 would be the same as T_C^+. In a real heat exchanger, the two fluids have different temperatures, with the fluid being cooled at a higher temperature than the fluid being heated. The finite temperature difference between

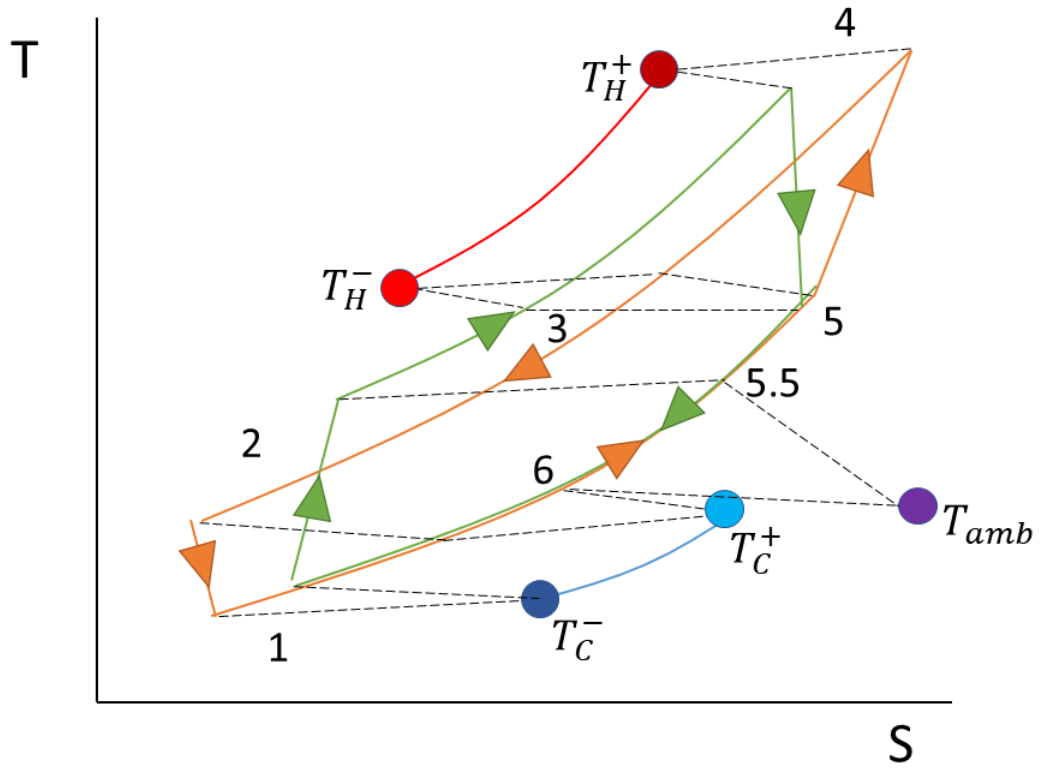

Figure 2-1: Real Thermal Storage Cycle T-S Diagram

the fluids is approximately constant through the device, and is referred to as an approach temperature. In the ideal cycle, the approach temperature is zero. On a T-S diagram, a nonzero approach temperature is included by offsetting the storage media temperatures from the working fluid temperatures. For example, the temperature at location 1 is lower than T_C^- in the heat pump mode and higher than T_C^- in the heat engine mode. The dashed lines showing the heat exchange are now sloping rather than horizontal.

A third difference for the real cycle is stagnation pressure loss in the heat exchangers. The ideal cycle has constant pressure heat addition through the heat exchangers, while the real cycle includes a pressure decrease in the heat transfer processes. For example, the pressure at location 4 is lower than location 2 in the heat engine mode, but higher in the heat pump mode. The result is that the pressure ratio is not the same through the cycle. In both charge and generation modes, the compressor has a higher pressure ratio than the turbine.

All of these irreversibilities in the real cycle contribute to waste heat that must be rejected to the environment. In the configuration of a thermal storage cycle shown here, the heat rejection step is placed between the cold storage heat exchange and the regenerator in the generation mode heat engine, between locations 5.5 and 6. It is placed here because T_C^+ is normally close to ambient temperature, making it easy to reject heat to the environment.

As with the ideal cycle, the real cycle is defined by two parameters: the pressure ratio and the normalized temperature difference between hot storage and ambient. The normalized temperature difference is set by the choice of storage media. Unlike the ideal cycle however, the pressure ratio is not the same everywhere in the real cycle. Not only do compressors have higher pressure ratios than their corresponding turbines, but the charge and generation directions have different mean pressure ratios. The pressure ratio across the turbomachinery is of most interest as it influences the turbomachine design, and by convention, the pressure ratio across the cold compressor is used to define the cycle because it is the largest pressure ratio of the four turbomachines.

To illustrate how the irreversibilities change the thermal storage cycle and thus impact RTE, we now assess the effects of turbomachine losses. Understanding the relationship between turbomachine losses and RTE will help to frame the considerations of turbomachine design. Figure 2-2 shows a T-S diagram with the only irreversibilities being those from turbomachine losses, with zero heat exchanger approach temperature and zero heat exchanger stagnation pressure losses.

We examine the two hot turbomachines first to show how the losses affect their performance. The temperature difference, and thus the work, across the hot machine is the same as the hot storage temperatures, T_H^- and T_H^+. The work across the hot machine (between stations 4 and 5) is therefore the same in both directions. To produce a given amount of work, the turbine from the heat engine requires a higher pressure ratio than in the ideal cycle. For a given amount of work, the compressor in the heat pump produces a lower pressure ratio than in the ideal cycle. As a result, the pressure ratio across the hot turbine is higher than the pressure ratio across the

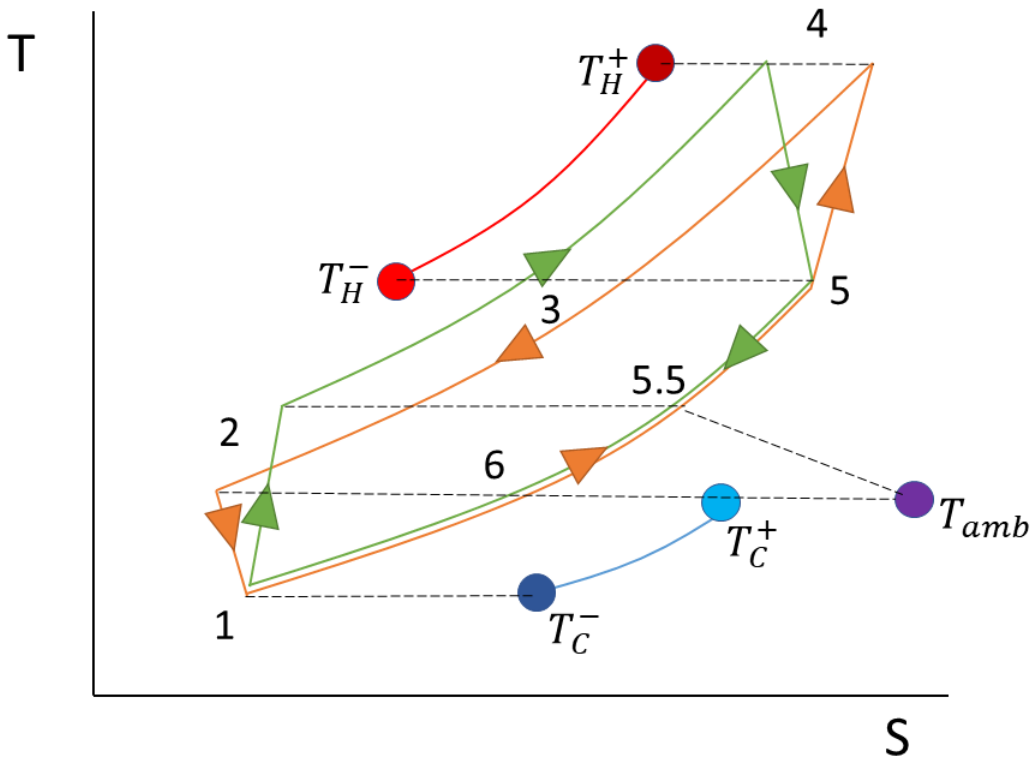

Figure 2-2: T-S Diagram of Thermal Storage Cycle with only Turbomachine Losses

hot compressor. On the T-S diagram, losses tilt the hot machine compression and expansion steps away from vertical, so each has a different pressure ratio. At the cold end of the cycle, to reach the higher pressure ratio of the heat engine, the cold compressor requires more work. Given the lower pressure ratio of the heat pump, the cold turbine produces less work. The result is that in generation mode, the cold compressor does more work than the cold turbine produces in charge mode. The difference in work between cold compressor and cold turbine is equal to the waste heat rejected to the environment. As turbomachine losses increase, and the compression and expansion steps on the T-S diagram tilt further from vertical, the work difference between the two cold turbomachines grows, more waste heat is rejected, and the round-trip efficiency drops.

2.2 Cycle Sensitivities

To understand the relationship between round-trip efficiency and the properties of each component in more detail, we have carried out a sensitivity analysis in which different cycle parameters (turbomachine efficiency, pressure ratio, and normalized temperature difference) are varied in turn. We first consider the effect of individual turbomachine efficiencies on RTE. Figure 2-3 shows RTE as a function of turbomachine efficiency, assuming all four turbomachines have the same efficiency. Two situations are illustrated: (i) the effects of turbomachine efficiency in isolation, such that they are the only sources of loss in the storage cycle, and (ii) the effects of turbomachine efficiency including the heat exchangers and stagnation pressure losses in stationary components. Values for stagnation pressure loss and heat exchanger approach temperature are taken from previous heat exchangers designed by Brayton Energy LLC [10].

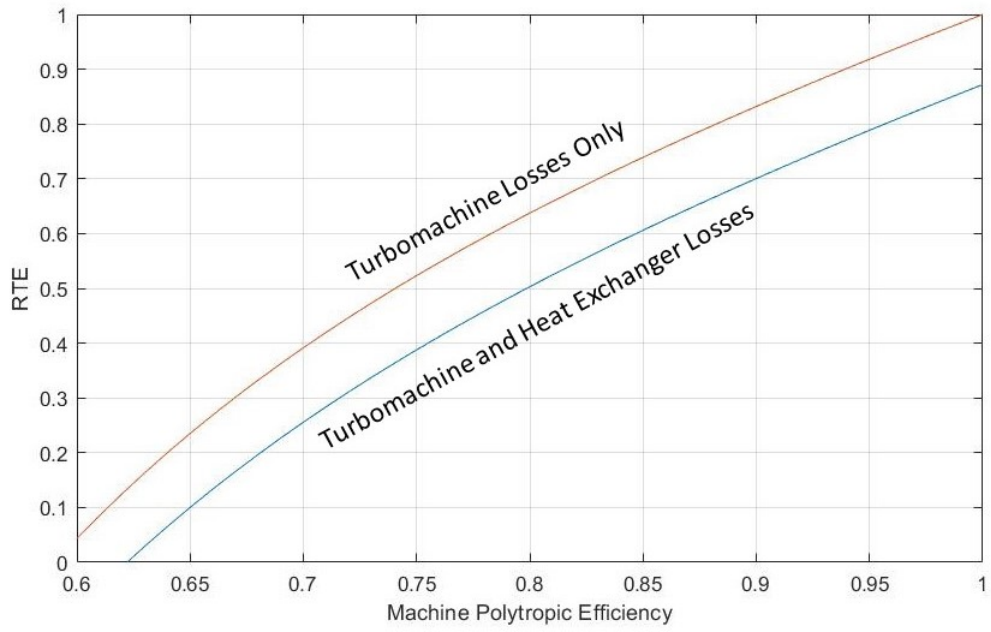

Figure 2-3: RTE vs. Turbomachine Efficiency With and Without Heat Exchanger Losses

Two observations are drawn from Figure 2-3. First, RTE becomes more sensitive to turbomachine efficiency as the turbomachine efficiency decreases. Improving the

turbomachine efficiency from 84% to 85% gives a higher RTE improvement than increasing turbomachine efficiency from 94% to 95%. Second, the sources of additional loss reduce RTE but do not change the sensitivity of RTE to turbomachine efficiency.

The round-trip efficiency is also dependant on the cycle pressure ratio. Figure 2-4 shows how RTE varies with the pressure ratio across the cold compressor. The turbomachine efficiencies have been set to 90% and the non-ideal effects of heat exchangers and stagnation pressure losses in stationary components are included.

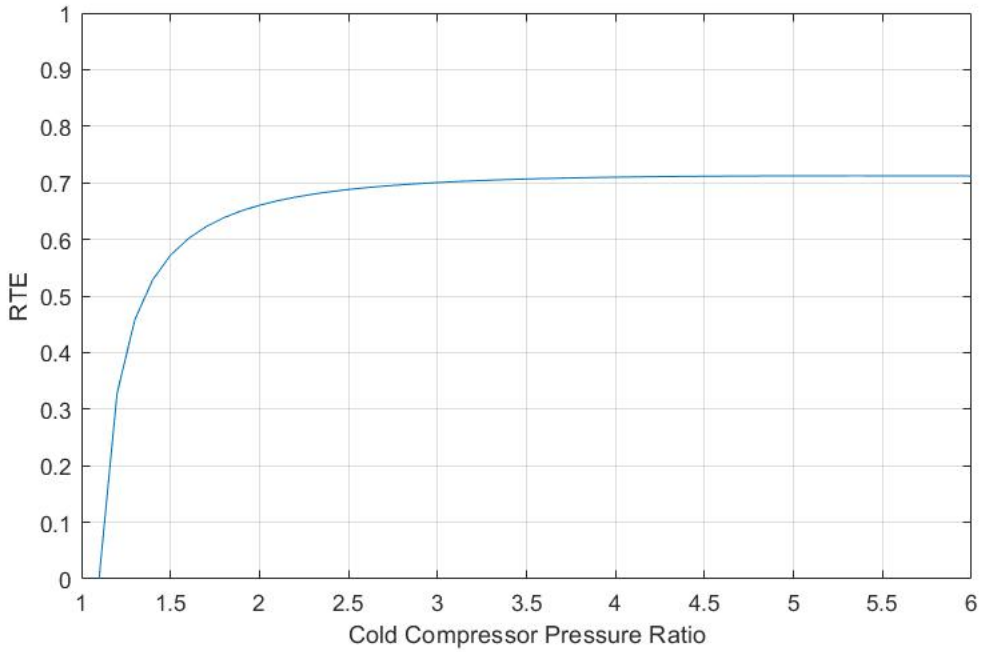

Figure 2-4: RTE vs. Cold Compressor Pressure Ratio, Including Non-ideal Heat Exchangers, and 90% Turbomachine Efficiencies.

Figure 2-4 shows that a higher cycle pressure ratio gives a higher RTE for the given turbomachine efficiency, up to about 3.5, beyond which RTE doesn't change. Figure 2-5 however, shows how RTE varies with pressure ratio for different values of turbomachine efficiency. At lower turbomachine efficiencies, RTE actually decreases with pressure ratio. RTE only increases with pressure ratio if the turbomachine efficiency is higher than about 85%. At lower values of turbomachine efficiency, below 85%, there is a pressure ratio which maximizes RTE, above which RTE decreases. In the design case assessed in this thesis, the turbomachine efficiency is high enough

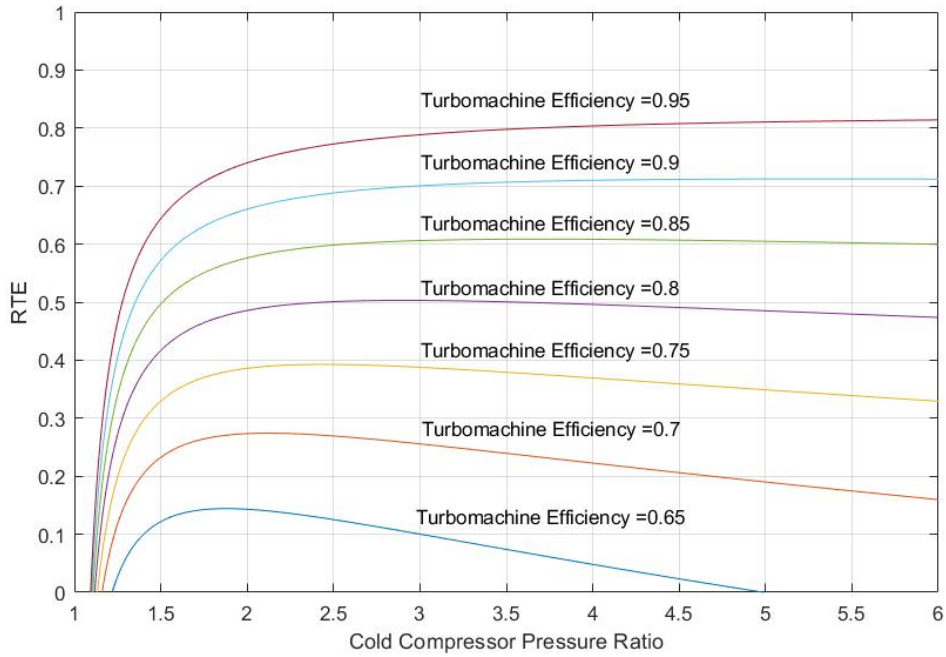

Figure 2-5: RTE vs. Cold Compressor Pressure Ratio for Different Turbomachine Efficiencies

that increasing the pressure ratio improves RTE.

The final parameter we assess in this section is the normalized difference between hot storage and ambient temperatures; $\frac{T_H^+ - T_{amb}}{T_{amb}}$. Larger normalized temperature difference gives a higher RTE no matter the turbomachine efficiency or heat exchanger performance. Figure 2-6 shows how RTE varies with the normalized temperature difference, for different values of turbomachine efficiency. A greater temperature difference always gives a higher RTE.

In summary, the round-trip efficiency is sensitive to the individual turbomachine efficiencies with approximately a factor of two of changes in the former for a given change in the latter. This sensitivity increases as turbomachine efficiency decreases. Additionally, for typical designs, a higher cycle pressure ratio gives a higher RTE, depending on the turbomachine efficiency. Finally, in all cases, a greater normalized temperature difference gives a higher RTE.

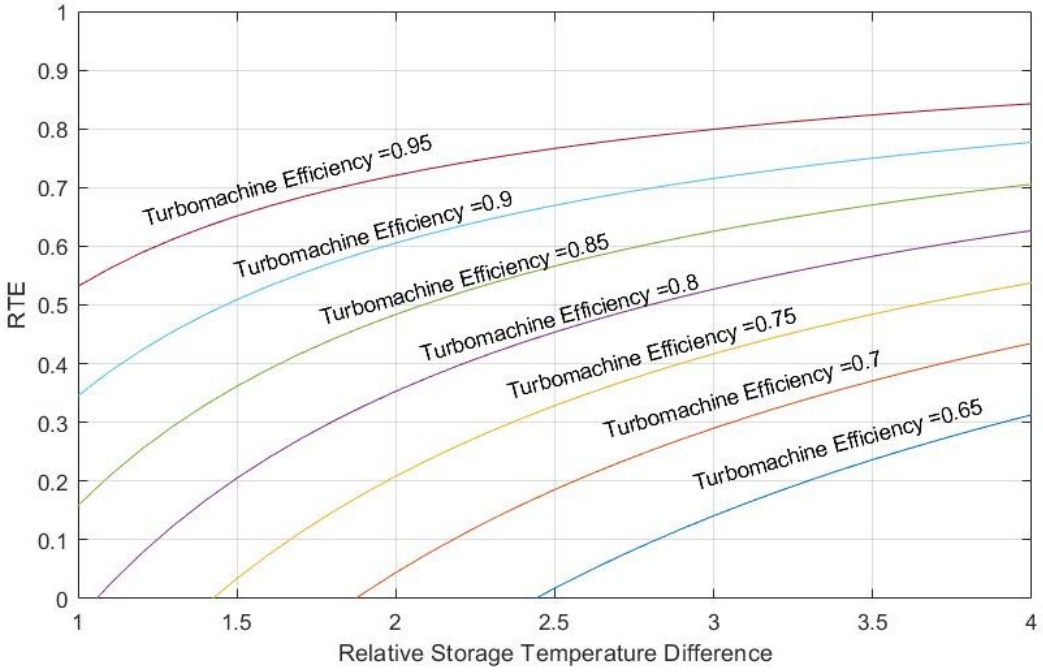

Figure 2-6: RTE vs. Normalized Temperature Difference for Different Turbomachine Efficiencies

THIS PAGE INTENTIONALLY LEFT BLANK

Chapter 3

Unique Requirements For Bi-Directional Turbomachinery

The requirements for a bi-directional turbomachine in pumped thermal energy storage are unique. There are some obvious requirements such as using airfoils which are efficient for flow in both directions, but there are other important requirements which may be less evident but also constrain the design space. The two described in this section are the non-symmetric[1] loading, because the cold machine does more work as a compressor than as a turbine, and the necessity for non-repeating stages in at least one direction of operation.

3.1 Cold Machine Non-Symmetry

The cycle defining pumped thermal energy storage involves a Brayton cycle and reverse Brayton cycle. With no losses, these two cycles overlap exactly and the aerodynamic loading across the turbomachines is the same in both directions. On the T-S diagram in Figure 1-5, the temperature at location 1 is the same for operation in both directions, and the temperature at location 2 is the same for operation in both directions. With losses however, the heat pump and heat engine cycles move

[1]The term, "non-symmetric" is used here to describe a behavior which is different for operation in one direction than in the other

apart, and the loading is no longer the same in both directions. Specifically, the cold machine does more work as a compressor than as a turbine. The relationship between the turbomachine efficiencies and the required work can be expressed compactly if we consider only losses associated with the turbomachines, and ignore heat exchanger and pressure drop losses. If so, the temperature ratios across the cold machine as compressor and as turbine are defined in Equations 3.1 and 3.2 as,

$$\tau_{CC} = \tau_{HT}^{\frac{1}{\eta_{CC}\eta_{HT}}} \tag{3.1}$$

$$\tau_{CT} = \tau_{HC}^{\eta_{CT}\eta_{HC}} \tag{3.2}$$

The subscripts CC, CT, HC, and HT refer to the cold compressor, cold turbine, hot compressor, and hot turbine, respectively. Equation 3.1 applies to the Brayton cycle heat engine and relates the temperature ratios across the cold compressor and the hot turbine. Equation 3.2 applies to the reverse Brayton cycle heat pump and relates the temperature ratios across the cold turbine and hot compressor. Because the hot machine has the same temperature ratio in both modes of operation, as shown in Figure 2-2, the cold machine temperature ratios are related to each other by

$$\tau_{CT} = \tau_{CC}^{\eta_{CC}\eta_{HT}\eta_{CT}\eta_{HC}} \tag{3.3}$$

Put simply, as the turbomachine efficiencies decrease from unity, the temperature ratio across the cold machine functioning as a turbine becomes less than the temperature ratio across the cold machine functioning as a compressor.

For blade design, the non-symmetric loading gives a second design requirement. Not only must the airfoils be efficient for flow in both directions, but the work, and therefore the flow turning for a given mass flow, must also be different for each direction. Two ways to address this requirement are to use different rotation rates in each direction and to use variable stators, as are in common use today in both aviation and ground-based gas turbines. The focus of this thesis however, is to develop an estimate of the best performance for counter-rotating bi-directional turbomachines in a PTES

system. The rotation rate is therefore fixed at 3600 RPM, to be synchronized with the electric grid, and variable vanes cannot be used because counter-rotating turbomachines have no stators. The different amounts of turning therefore, are achieved with different incidence angles, as we will see in the following. For now, we also assume the turbomachine operates with repeating stages in both directions. This assumption does not hold true for a real bi-directional turbomachine, but it is used here as a helpful simplification to highlight the effects of non-symmetric loading.

For any given work coefficient, $\Delta h_t/U^2$, in compressor mode, there is a matching work coefficient in turbine mode which fulfils the non-symmetric loading requirements from the cycle. For a given blade geometry, the pair of work coefficients correspond to a pair of incidence angles. If we were to increase the incidence angle of one mode of operation, the corresponding incidence angle in the opposite direction would also increase. To find the best operating point, we need to identify the pair of incidence angles where round-trip efficiency (RTE) is maximized, rather than the angles where either individual turbomachine efficiency is maximized on its own. To illustrate the point, Figure 3-1 shows the stage efficiency vs incidence angle curves for an example double-circular-arc blade calculated using the 2D CFD code, MISES [7]. The points denoted by green circles are the pair of incidence angles at which RTE is maximized.

In neither the compressor nor the turbine mode does the turbomachine operate with maximum efficiency, because maximum RTE is achieved with a balance between compressor and turbine efficiency. If we wish to improve turbine efficiency, by increasing incidence, compressor efficiency would decrease, as its incidence also increased.

This issue would not arise if the efficiency vs incidence curves for both turbine and compressor modes were flat. If so, the turbomachine would be able operate with maximum efficiency in both directions. A round-trip efficiency calculated using such turbomachine efficiency values represents what the RTE could be *if the performance in both directions were independent of incidence* or if two individual turbomachines were used for compressor and turbine, each operating at their own maximum efficiency. The difference between a (fictitious) RTE for these situations, and the real RTE, as calculated with the efficiency curves in Figure 3-1, is therefore the penalty paid by

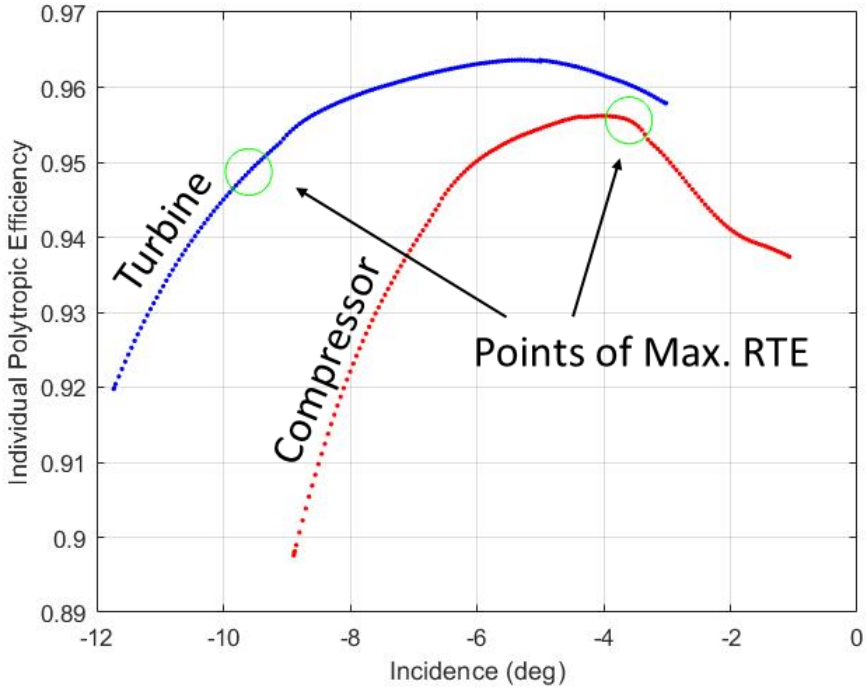

Figure 3-1: Compressor and Turbine Individual Efficiency vs. Incidence for Double Circular Arc Airfoil, Re=2.6E6

using a single bi-directional turbomachine as both compressor and turbine.

The difference in compressor and turbine aerodynamic loading is a function of the individual turbomachine efficiencies according to Equation 3.3. Knowing that aerodynamic loading is linked to flow turning, Equation 3.3 also shows that the difference between compressor and turbine incidence angels is a function of the turbomachine efficiencies. We can estimate this RTE penalty as a function of individual turbomachine efficiency by adding a constant loss to the two-dimensional value calculated by MISES, shifting the efficiency curves from Figure 3-1 vertically. Doing so allows us to determine what would happen if turbomachines with poorer efficiency were used, as shown in Figure 3-2. The dashed curve, labeled "fictitious RTE", is the value calculated as if the efficiency vs. incidence curves were flat. The solid curve, labeled as Matched RTE, is the RTE based on the efficiency values at the incidence angles where the cycle requirements are met. The difference between these is the RTE penalty. RTE values are plotted as a function of Peak Compressor Efficiency, which is the maximum value of turbomachine efficiency for the compressor.

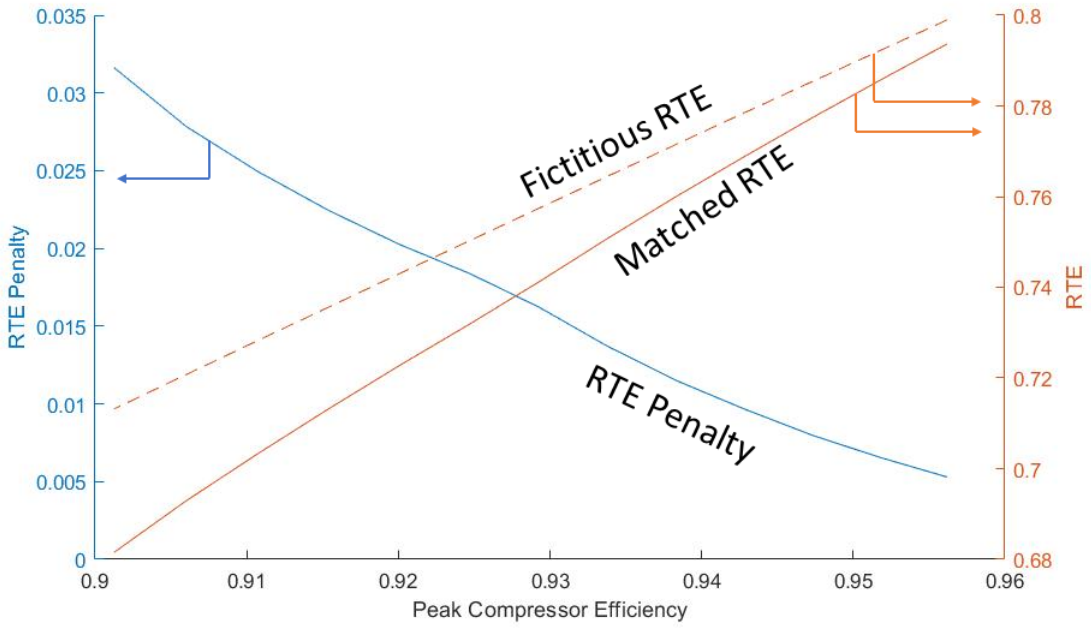

Figure 3-2: RTE Penalty due to Non-Symmetric Loading Requirements

As the individual turbomachine efficiencies are lowered, the difference in loading between operation as a compressor and as a turbine grows. In Figure 3-1, this would be indicated by the green points moving apart. The result is that a less efficient turbomachine will operate even further from its own maximum efficiency. High efficiency turbomachines are necessary for a high RTE in a PTES system, but with bi-directional turbomachines, this necessity is doubly important. Not only does the fictitious RTE fall with turbomachine efficiency, but the RTE penalty grows as well. The matched RTE is thus more sensitive to turbomachine efficiency when using bi-directional turbomachines compared to single direction turbomachines.

3.2 Non-repeating Stages

The second unique requirement placed on bi-directional turbomachines is that the turbomachine cannot have repeating stages in both directions. This requirement does not necessarily have a negative impact on RTE, but it uniquely constrains the design space.

Repeating stages is a useful assumption to make in initial turbomachine design

and may indeed be a useful design choice. With the bi-directional turbomachines proposed however, it is impossible to have repeating stages in both directions. Unless a variable area system were part of the design, the height of the passage is the same for both directions. For repeating stages, as flow progresses through the compressor, the density increases across each stage, and the passage height decreases so the axial velocity is constant. The reverse happens through a turbine, where the passage height increases so the axial velocity is constant as density falls. The rate at which the passage height increases or decreases is determined by the density change through the turbomachine, which is related to the turbomachine work. As described in the first half of this section, the PTES thermodynamic cycle requires the cold turbomachine to do more work as a compressor than as a turbine, so the density change through the compressor is greater than the density change through the turbine. If the passage heights are set to give repeating stages in one direction, they thus cannot give repeating stages in the other.

The approach taken here to address this issue is to implement repeating stages as a compressor, and non-repeating stages as a turbine. The rationale is that compressors are typically more sensitive to incidence angle variations than turbines. In turbines, the performance degrades less with variations in incidence angle than do compressors.

An example design, with 9 rotors, based on this approach is shown in Figure 3-3, which shows the same efficiency curves as Figure 3-1, but denotes the incidence angle at each rotor. The compressor uses repeating stages, so the incidence angle is the same, and all points stack up on one another. The turbine stages each have a different incidence angle determined by the density change and the passage heights set by the compressor mode. The forward turbine rotors have higher incidence and thus a higher efficiency than do the aft rotors, which have large negative incidences and thus lower efficiency. In this case, the overall turbomachine efficiency is slightly higher than if repeating stages could have been used. Section 5.1 goes into more detail on the implications of non-repeating stages in turbine mode and how best to design for it. Here it is sufficient to say that any bi-directional turbomachine used in a PTES system must have non-repeating stages in at least one direction of operation.

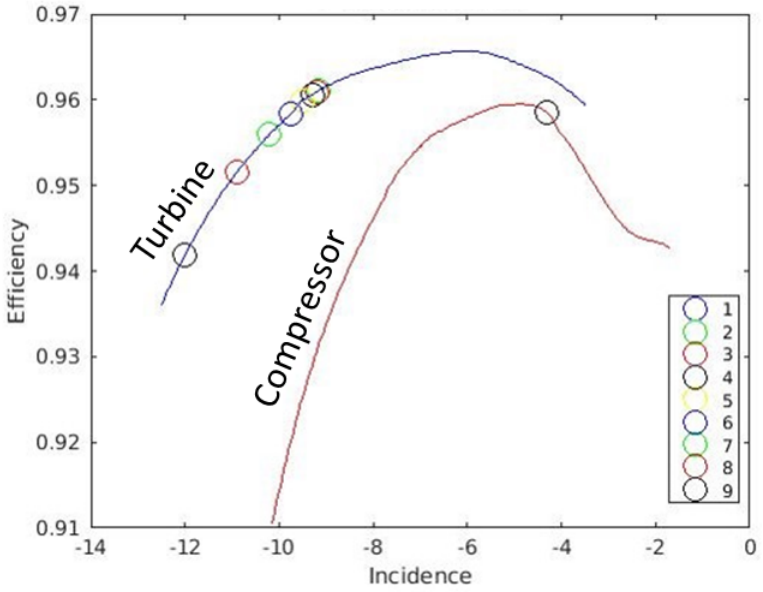

Figure 3-3: Individual Efficiency Curves with Non-Repeating Turbine Stages

THIS PAGE INTENTIONALLY LEFT BLANK

Chapter 4

Design Concept

In Chapters 2 and 3 we describe the pumped thermal energy storage (PTES) cycle, how the turbomachinery impacts round-trip efficiency (RTE), how a bi-directional turbomachine can be used in the PTES cycle, and what unique requirements are associated with it. To address these unique requirements, in Chapter 5 we develop several design principles for bi-directional turbomachines. These principles are developed using Brayton Energy LLC's 50MW bi-directional turbomachine design as an architecture, within which several two-dimensional design features for the cold machine are assessed. This chapter describes the details of Brayton Energy's 50 MW architecture and the reasoning for focusing on two-dimensional design features in the cold machine.

4.1 Turbomachine Architecture

In conjunction with the research presented in this thesis, Brayton Energy LLC is designing bi-directional turbomachines for a 50MW PTES system, used in Chapter 5 as an architecture within which several design features are assessed. The turbomachines in the Brayton Energy system are counter-rotating, with no stators between rotors. The baseline design of the cold machine has 9 rotors with a pressure ratio of 3.5 for the heat engine. There are variable vanes at the inlet and exit to control the mass flow in each direction. The system is synchronized with the electric grid, with the

turbomachines rotating at a fixed rate of 3600 RPM in both directions to match the 60 Hz frequency of the U.S. electric grid. In Europe, the turbomachines would be designed to rotate at 3000 RPM to match the 50 Hz frequency of the European grid.

Counter-rotating turbomachines offer a potential size benefit compared to non-counter-rotating turbomachines. In a power application, the rotors are synchronized with the electric grid and rotate at a fixed speed of 3600 RPM. Counter-rotation effectively doubles the blade speed for the same mean radius and rotation rate, so counter-rotating turbomachines can be smaller than conventional turbomachines of equivalent power. Offsetting this benefit, however, is that counter-rotating turbomachines do not have stators, and cannot use variable vanes between rotors. As discussed in Section 3.1, the non-symmetric loading requirement for the turbomachinery must be addressed by using different incidence angles in each direction.

4.1.1 Connection of Counter-Rotating and Conventional Turbomachines

The design guidelines discussed in this thesis are developed for counter-rotating bi-directional turbomachines. Conventional-rotating bi-directional turbomachines however, are aerodynamically similar to counter-rotating turbomachines if certain corrections are made [13].

The conventional definitions of flow coefficient and work coefficients are

$$\phi = c_x/U \tag{4.1}$$

$$\psi = \Delta h_t/U^2 \tag{4.2}$$

These definitions apply to both counter-rotating and conventional-rotating turbomachines, but the definition of blade speed, U, is different in the two cases. In a conventional-rotating turbomachine, U is the tangential speed of the rotor. In a counter-rotating turbomachine however, U can either refer to the rotational speed of a given rotor relative to a stationary reference frame, or the rotational speed of a given

rotor relative to an adjacent rotor. With rotors of equal but opposite rotational rates, this doubles the rotor speed, halving the flow coefficient and quartering the work coefficient.[1] A helpful way to visualize the connection is to consider a counter-rotating turbomachine from a rotating frame of reference fixed to every other blade row. In this view, the turbomachine appears identical to a conventional turbomachine with twice the rotation rate.

The definition of a stage is also different. In a conventional-rotating turbomachine, a *stage* refers to a pair of blade rows, a rotor and stator. In a counter-rotating turbomachine, a *stage* could refer to a single rotor, or a sequential pair of rotors. If a single rotor is taken as a stage, it is appropriate to adjust the work coefficient correspondingly; if the reaction is 50%, the work coefficient is doubled to account for the second rotor.

The reason for using a rotating frame of reference is that conventional and counter-rotating turbomachines can be directly compared. If two turbomachines had identical blade profiles, they would only have the same work and flow coefficients if the counter-rotating turbomachine considered a pair of rotors as a stage and defined U by the rotation rate of one rotor relative to the adjacent rotor. The design principles presented in Chapter 5 are developed using a counter-rotating architecture. A bi-directional counter-rotating turbomachine however, is aerodynamically equivalent to a bi-directional conventional-rotating turbomachine with twice the radius. The guidelines presented in Chapter 5 therefore, should work with bi-directional conventional-rotating turbomachines as well.

Brayton Energy has employed the convention that work and flow coefficients are defined by a single rotor, with respect to a stationary reference frame. In this thesis, to prevent confusion, numerical values for flow and loading coefficients are avoided. We will instead define blade shapes by their metal angles.

[1]Note that quartering the work coefficient only works for repeating stage turbomachines. If the swirl angle changes across the stage, then the work from the rotating reference frame must be included.

4.2 Design Focus

The design guidelines suggested in this thesis are focused on the cold turbomachine, which is the compressor in the Brayton cycle heat engine and the turbine in the reverse Brayton cycle heat pump. This turbomachine operates between points 1 and 2 on the system schematic in Figure 1-4 and in the T-S diagram in Figure 1-5. The focus is on the cold machine because, as discussed in Section 3.1, it has more challenging requirements than the hot machine. The cold machine must do more work as a compressor than as a turbine, which forces it to operate below its maximum efficiency in both directions. The hot turbomachine, which does the same work in both directions, can operate closer to its maximum efficiency, in both directions, compared to the cold machine.

The cold machine guidelines given in Chapter 5 are limited to 2D design features. A decision was made to focus on the 2D details of a bi-directional blade, allowing us to give more attention to the effects of incidence angle, and the non-symmetric loading requirement described in Section 3.1. Additionally, 3D flow calculations done by Brayton Energy [11] indicate that approximately 70% of the losses are attributable to the 2D blade profile. Specifically, using a tangentially averaged, spanwise distribution of efficiency, the loss value at the meanline was 70% of the average loss value in the passage. It was decided therefore, that focusing on the 2D design of a bi-directional turbomachine would provide the most useful learnings.

4.2.1 High Dependence of Loss to 2D Blade Design

The figure of 70% of the losses being attributable to the 2D blade profile. is higher than would be expected for most aero engine turbomachinery, such as the loss breakdowns given by Cumpsty [1] or Hall [8], especially for turbines. There are two reasons for this. First, tip clearances on the hub-mounted blades are small, ranging from 0.3% to 0.6% of the blade span, (Hall's loss breakdown uses a tip clearance of 1.0% of blade height) implying that tip losses are smaller for this turbomachine than typical aero engines. Second, the casing-mounted rotors are shrouded at both ends and have no

tip clearance. There is no hub clearance either, as a blade-mounted shroud with a labyrinth seal is used. With this in mind, the high dependence of losses on 2D design features in this turbomachine makes sense. There are, however, non-2D aspects of the design which are not considered in Chapter 5, but may be a useful topic for future work.

THIS PAGE INTENTIONALLY LEFT BLANK

Chapter 5

Design Features and Results

In this chapter we use the turbomachine architecture described in Chapter 4 and the unique requirements identified in Chapter 3 to identify best design practices for a bi-directional turbomachine. The discussion of the bi-directional turbomachine design will be divided into 3 categories: the number of stages in Section 5.1, the meanline velocity triangles in Section 5.2, and the 2D profile of the blades in Section 5.3.

5.1 Stage Count

The number of turbomachine stages is linked to the chosen pressure ratio for the thermodynamic cycle. The question is "given a particular pressure ratio, how many stages is best for this application?" In assessing this, the analysis here focuses on the relationship between round-trip efficiency (RTE) and number of stages.

The *stage count* for the counter-rotating turbomachine is defined as the number of turbomachine blade rows. In these terms a 9-stage turbomachine means 9 rotors, 4 rotating in one direction and 5 in the other. Pressure ratio and stage count serve as initial design parameters, with pressure ratio defining the cycle and stage count defining the turbomachine.

Two effects dictate the relationship between efficiency and stage count. The first is that for a given pressure ratio, the Mach number relative to the blade decreases with increased stage count. A lower relative Mach number reduces the minimum

profile loss of the blade row, allowing the turbine and compressor incidence angles to be closer to those of maximum efficiency. Reducing the relative Mach number is similar to moving to the right on the chart in Figure 3-2.

The second effect is the requirement for non-repeating stages (Section 3.2). With blade heights set by compressor operation, there are non-repeating stages in turbine mode, and each rotor has a different incidence angle, with the front rotors having less negative incidence than the rear rotors. The turbine incidence angles translate to differences in stage efficiency through the turbomachine; the front rotors have higher efficiency by up to 2 percentage points compared to the rear rotors. Of the two effects, loss reduction due to lower relative Mach numbers is dominant.

The effects due to stage count were evaluated using the MISES code [7] and a MATLAB model of the thermal cycle. The metric is the round-trip efficiency (RTE), which includes both cycle properties and turbomachine efficiencies. Figure 5-1 shows how RTE changes with stage count for three different compressor pressure ratios. The x-axis is stage count, the y-axis is RTE, and the curves are for pressure ratios of 3, 4, and 5. Each stage count was assessed for multiple values of stage loading, and the highest RTE from the assessment is shown.

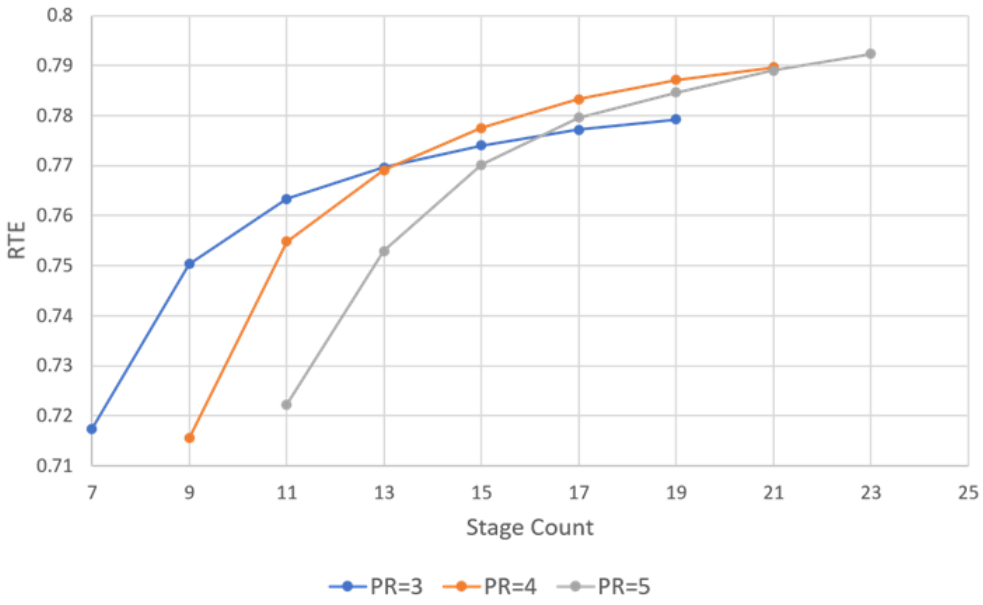

Figure 5-1: RTE vs. Stage Count for Different Cycle Pressure Ratios

Figure 5-1 indicates turbomachines with more stages (rotors) have higher RTE, primarily because of lower relative Mach number. Increasing the pressure ratio can increase RTE, but only if the number of rotors is also increased. As discussed in Section 2.2, a higher pressure ratio raises RTE. For a given stage count however, increasing the pressure ratio also increases the relative Mach number. The stage count therefore, needs to be increased to achieve the benefits of a higher pressure ratio.

5.2 "Smith Chart" for Bi-Directional Turbomachines

The loading and flow coefficients of a two-dimensional turbomachine blade row are defined by the inlet and exit flow angles. Charting the efficiencies of turbomachines in terms of their respective loading and flow coefficients provides useful trends in the design space. Such a chart, known as a *Smith chart*, was originally developed for measuring the performance of turbines [4], but the process has been applied to compressors as well [3].

We wish to map out the 2-D design space of a bi-directional turbomachine analogous to a Smith chart. A challenge exists because of the difference from a single-direction Smith chart, which considers the turbomachine maximum efficiency point. The bi-directional turbomachines of interest here cannot operate with maximum efficiency in both directions. To map out the design space of a bi-directional turbomachine in a manner analogous to a Smith chart, we need to account for the PTES thermodynamic cycle requirements which dictate that the turbomachine cannot have the same loading in both directions. We thus use the blade stagger and camber rather than flow coefficient and blade loading, noting that the camber is primarily related to the loading, and the stagger to the flow coefficient. The advantage from using stagger and camber is they are calculated using the metal angles; the blade geometry does not change between compressor and turbine modes.

A typical Smith chart uses polytropic or isentropic efficiency as a performance metric. Another difference for a bi-directional turbomachine is that the round-trip

efficiency, which combines both directions of operation, is the metric.

Based on these ideas, a bi-directional Smith chart was created using a series of double-circular arc blades with the efficiency found using MISES. Double-circular arcs are used because their fore-aft symmetry gives a starting point for bi-directional blade design. The assessment of each blade provides a chart similar to 3-1 with a round-trip efficiency for each geometry. As a first assessment, this process was carried out using incompressible flow calculations so that a large number of geometries could be rapidly assessed. Compressible calculations were then carried out for a narrower design space. A Smith chart of this type is given as Figure 5-2. The x-axis is stagger, the y-axis is camber, and RTE is shown as colored points according to the color bar scale. The results of Figure 5-2 show that a camber near 37 degrees and stagger near

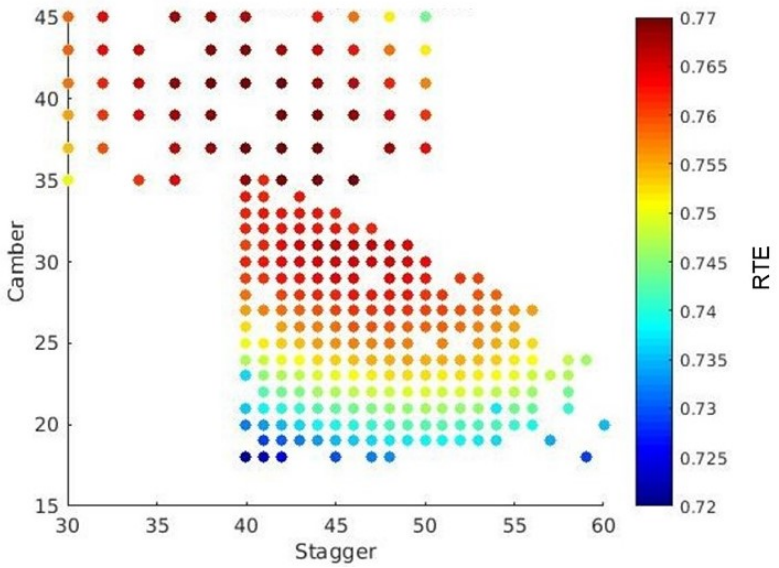

Figure 5-2: RTE vs. Camber and Stagger, Incompressible, Re=2.6E6

42 degrees gives the highest round-trip efficiency.

The cycle requirements dictate that the turbine does less work than the compressor, and it thus has a lower incidence angle. With double circular arcs, the best RTE was achieved with compressor incidence near 0 degrees, and turbine incidence near -12 degrees.

Figure 5-3 shows turbine incidence angles for each camber and stagger design assessed. The x-axis is stagger, the y-axis is camber, and turbine incidence is shown

as colored points according to the color bar scale. With increasing blade camber, the turbine incidence becomes more negative. For an application with non-symmetric

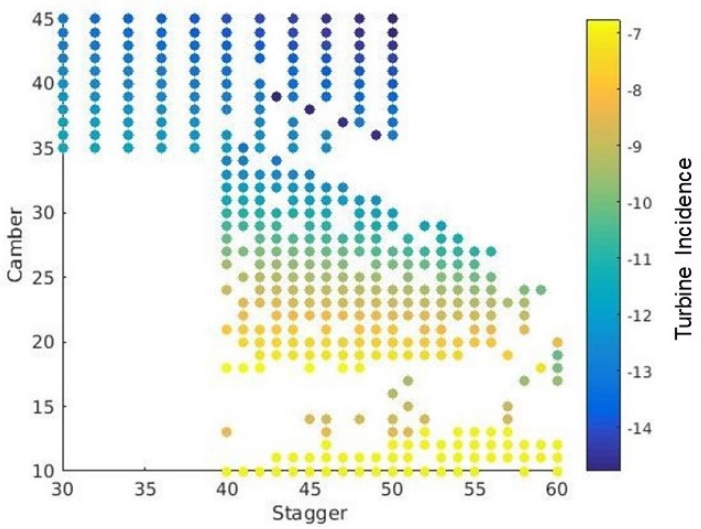

Figure 5-3: Turbine Incidence vs. Camber and Stagger, Incompressible, Re=2.6E6

loading, the turbine incidence is less than the compressor incidence. The compressor is more sensitive to high incidence than is the turbine to low incidence, so negative turbine incidence provides the highest RTE.

Another finding is that camber has a greater impact on RTE than does stagger. We thus simplify assessment of the design space by varying blade camber only, holding stagger constant. The resulting assessment is a vertical slice of the camber-stagger Smith chart from Figure 5-2. Making this simplification in the assessment process is useful for compressible flow calculations, which take more time to compute and need to be repeated across a range of Mach numbers.

Compressibility is addressed with the methods discussed in Section 5.1, where stage count, pressure ratio, and relative Mach number are linked. Each proposed number of stages has been assessed for blades with camber ranging from 23 to 39 degrees, in 2 degree increments, at a stagger of 42 degrees. The results in figure 5-4 show the camber that achieves the highest RTE at each stage count for 3 different pressure ratios. The x-axis is stage count, the y-axis is camber for highest RTE, and the curves show pressure ratios of 3, 4, and 5. As long as there are at least 11 stages, a camber close to 33 to 35 degrees gives the highest RTE, no matter what the pressure

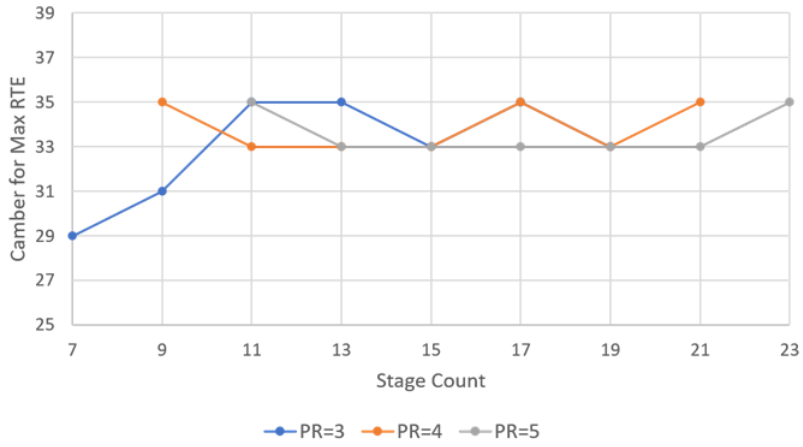

Figure 5-4: Camber For Highest RTE at Each Stage Count; Pressure Ratio = 3, 4, 5

ratio. With fewer than 11 stages, there was an increase in relative Mach number and a lower camber, close to 30 degrees was preferable. In every case examined, the selection of camber was less important than the selection of the number of stages.

Figure 5-5 shows a plot of RTE vs stage count for 4 different cambers. The information is similar to 5-1, except that each blade camber is separated into its own curve, and only one pressure ratio, PR=3, is shown for clarity, but other pressure ratios show the same message.

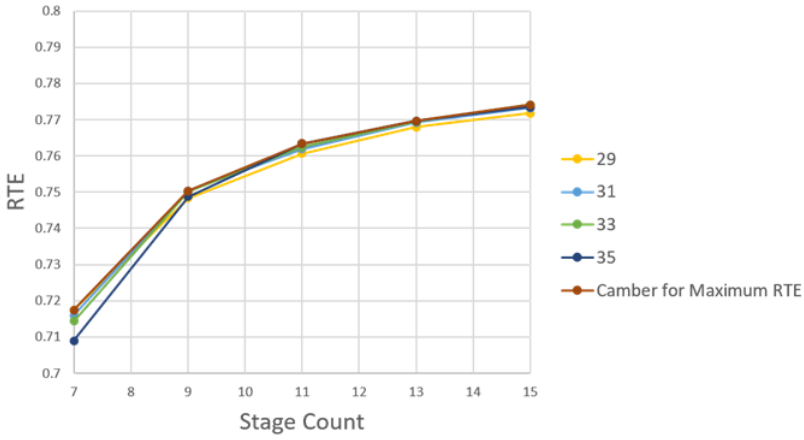

Figure 5-5: RTE vs. Stage Count; Camber = 29, 31, 33, 35

At each stage count, the 4 blade cambers are closely clustered and the RTE change from adding a stage is greater than the RTE change from choosing a new camber.

The interpretation is that for a bi-directional turbomachine, properly selecting the number of stages is most important; blade camber is secondary to stage count.

5.3 Blade Optimization

In Sections 5.1 and 5.2, double circular arc blades were used to assess the effects of stage count, camber, and stagger. Although these blades have fore-aft symmetry, there is no reason to assume a double-circular arc is best blade for a bi-directional turbomachine and we thus examine profile optimization to determine whether another geometry can achieve lower profile loss in both directions.

To carry out this examination, we used MILOP [5][1], an optimization program that works with MISES, to modify profile geometries to achieve a given goal. The starting blade is parameterized by a series of Chebyshev polynomials. The coefficients of the polynomial terms are then used as design parameters to perturb the shape of the blade surface, while maintaining a smooth shape without discontinuities. In addition to solving for the flow field, MISES calculates the flow field sensitivity to each polynomial coefficient, and, given this information, MILOP determines how best to adjust the design parameters to minimize profile loss.

The bi-directional design goal involves optimizing the blade shape for operation in both directions. To do this, the mode shapes associated with the Chebyshev polynomials are modified so the resulting blade shape is consistent when reversed. In other words, when the polynomial coefficients are modified, the perturbations to the original blade shape are applied in one direction for compressor mode, and in the opposite direction for turbine mode.[2] allowing the resulting blade not to be fore-aft symmetric.

The optimization was set up with 5 constraints: 3 thickness requirements and 2 flow turning requirements. The maximum thickness and the thickness at $x/c = 0.01$

[1]There is no documentation for MILOP. The documentation referenced here is for LINDOP, the airfoil optimization program, which is nearly identical to MILOP.

[2]The "tail-wagging" mode suggested by the MISES documentation was not used, as it could not be reversed to a "nose-wagging" mode for bi-directional flow.

and $x/c = 0.99$, where x/c is the position along the chord, are set to be the same as the double-circular arc starting blade. These 3 thickness requirements prevent the optimizer from selecting a shape with negative thickness, while still giving it freedom to find the best shape. To assess the impact that the thickness requirements have on RTE, each was adjusted in turn and the optimization repeated. The flow turning in both directions is held constant for each resulting blade design. This requirement ensures that, as the blade is modified, it will fulfill the cycle requirements. The inlet and outlet flow angles are set, with the blade geometry in-between allowed to vary. The goal was to minimize the sum of the entropy created in the compressor and turbine modes. With the work being held constant, this maximizes efficiency.

The starting point for the optimization is the 9 stage counter-rotating turbomachine with double circular arc blades introduced in Section 4.1. The 9 blades have 20.8° of camber and 42.3° of stagger at the meanline. The maximum thickness is 5.9% of chord and edge thicknesses at $x/c = 0.01$ and $x/c = 0.99$ are both 1.0% of chord. The Mach number is set by the conditions at Rotor 4 (counting in the compressor direction) which is used as a representative example from which an optimized blade can be generated. Rotor 4 is near the middle of the turbomachine and is hub-mounted. The resulting blade was then used in all 9 rotors, with repeating stages in compressor mode and non-repeating stages in turbine mode.

5.3.1 Optimized Blade Details

The optimized blade is shown in Figure 5-6, overlaid on the original double-circular arc. Two features distinguish the former from the latter. First, is the reduced camber in the optimized blade. Given that the inlet and outlet flow angles are the same for both airfoils, camber reduction means an increase in incidence and a decrease in deviation for the optimized blade. Second, although the maximum thickness, near mid-chord, is the same, the optimized blade is thinner approaching either edge.

The optimized blade reduces the compressor loss coefficient by 21%, from 0.0165 to 0.0130, and the turbine loss coefficient by 31%, from 0.0307 to 0.0212, for the fourth stage. The decrease in loss thus corresponds to an increase in 2D stage efficiency

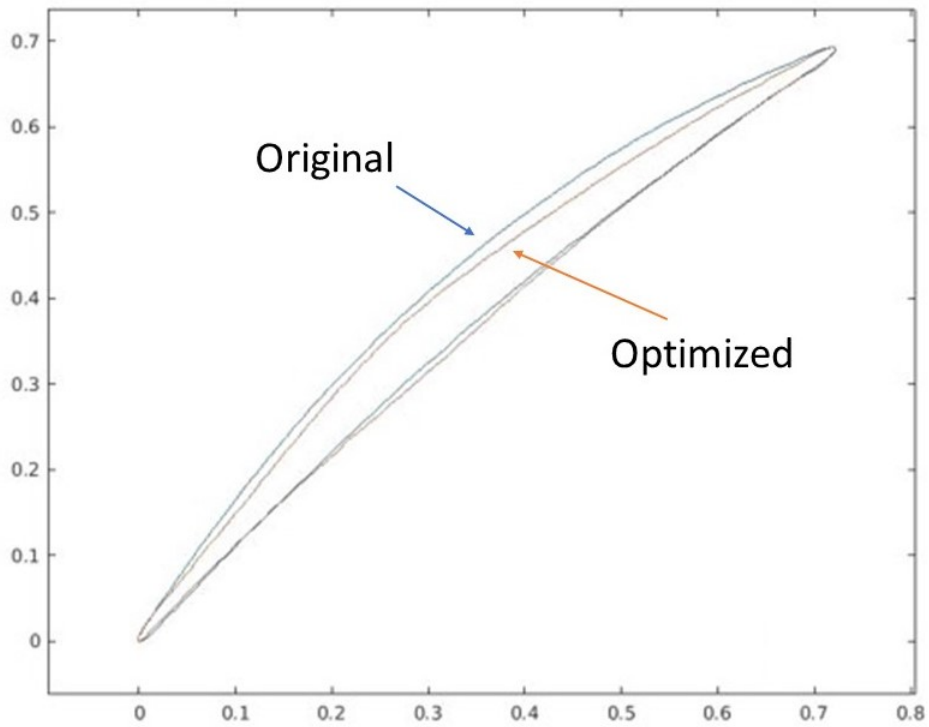

Figure 5-6: Optimized Blade Shape and Original Double Circular Arc Blade

of about 1 percentage point (from 0.952 to 0.963) for the compressor and about 3 percentage points (from 0.904 to 0.937) for the turbine. When the optimized blade is used in all 9 stages, the round-trip efficiency increases by 2.0 percentage points, from 0.764 to 0.784. The improvement comes from a reduction in deviation and reduced viscous losses in the trailing edge region of the suction surface and in the wake.

Figure 5-7 compares the dissipation coefficient on the suction surface of both airfoils in compressor and turbine modes. The dissipation coefficient is defined by Equation 5.1, where $\mathcal{D}$ is the local rate of kinetic energy dissipation into heat.

$$c_{\mathcal{D}} = \frac{\mathcal{D}}{\rho_e u_e^3} \tag{5.1}$$

In the trailing edge regions of the suction surfaces, as highlighted by the red ovals, the dissipation is higher for the original blade. In compressor mode, the optimized blade has a spike in dissipation at the suction surface leading edge, indicative of the higher compressor incidence angle of the optimized blade compared to the original blade.

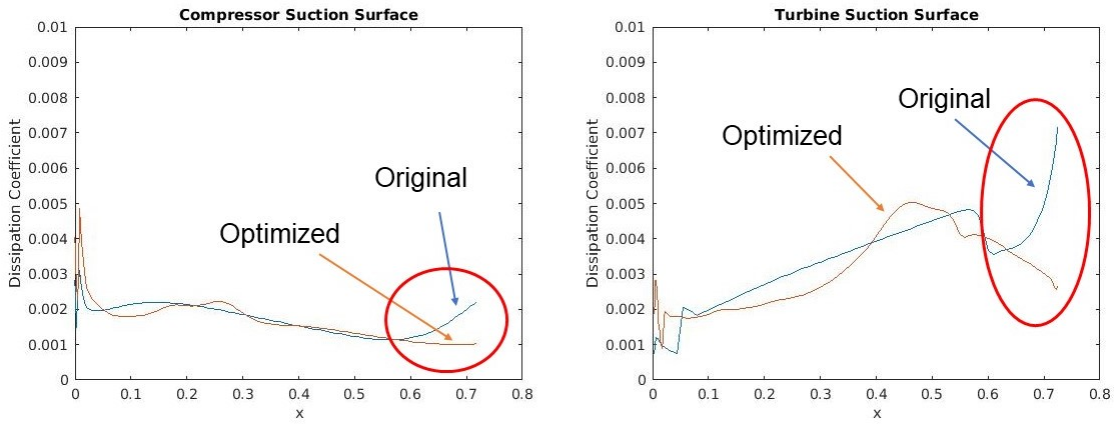

Figure 5-7: Suction Surface Dissipation Coefficients for Original and Optimized Airfoils

Near the leading edge therefore, the optimized blade has more dissipation, but, this occurs over a small region, and the overall loss is lower than the original blade. The increase in compressor incidence allows the turbine incidence to be less negative, so the optimized turbine pressure surface dissipation is lower than the original blade. The optimized pressure surface dissipation in compressor mode is similar to the original blade. The dissipation coefficient on the pressure sides are shown in Figure 5-8.

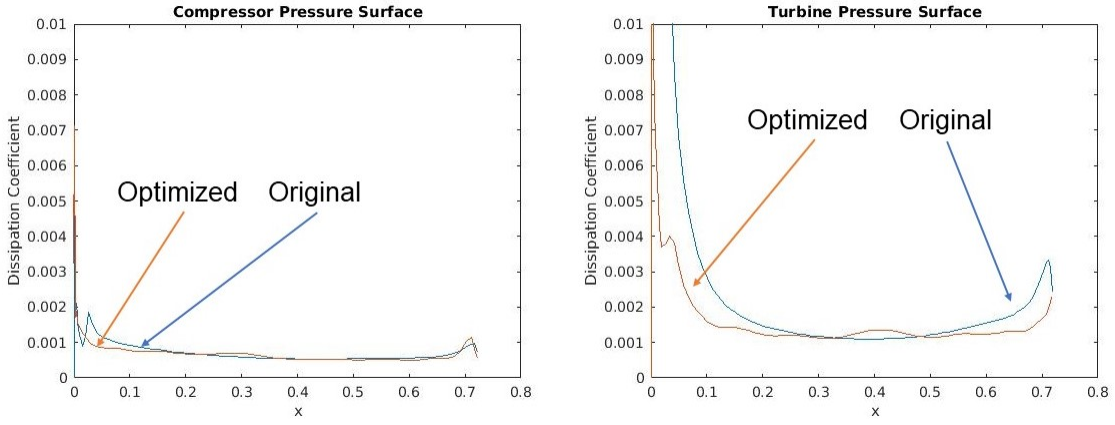

Figure 5-8: Pressure Surface Dissipation Coefficients for Original and Optimized Airfoils

The decrease in dissipation in the trailing edge region of the suction surface is achieved by shaping the blade so that the camber near both edges is decreased and more of the turning is done near mid-chord. Figure 5-9 compares the suction surface

Mach number distributions of the original and optimized airfoils in compressor and turbine modes to show aerodynamic loading in each. The red arrows in Figure 5-

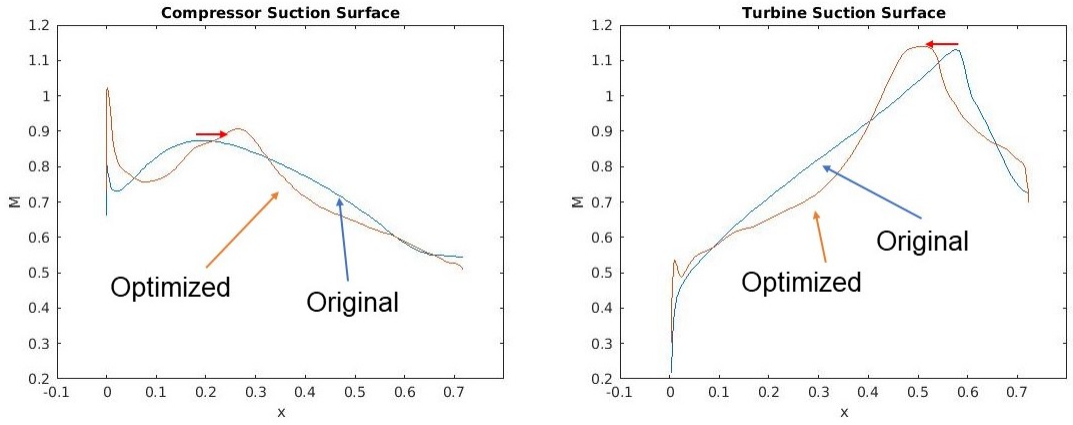

Figure 5-9: Surface Mach Number Distributions for Original and Optimized Airfoils

9 indicate that the peak Mach number is shifted towards the middle of the blade, so the pressure gradient aft of the Mach number peak is less adverse, producing a boundary layer less likely to separate [6]. The suction surface boundary layer shape factor shown in Figure 5-10 corroborates this observation. The original double circular

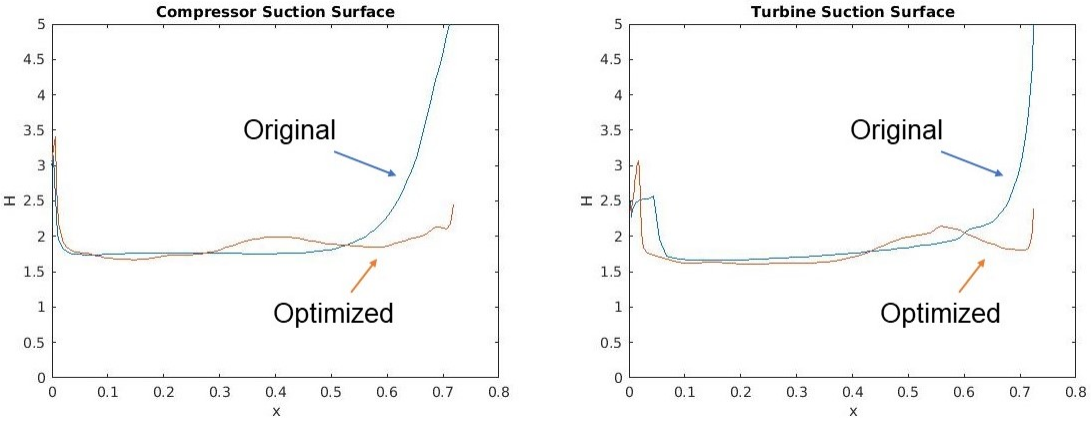

Figure 5-10: Boundary Layer Shape Factor for Both Original and Optimized Airfoils

arc blade produces a boundary layer with a higher shape factor than the optimized blade. Increasing flow turning at mid-chord increases the shape factor immediately aft of mid-chord compared to the original blade, but substantially lowers it in the trailing edge region.

In summary, the optimized airfoil has two main features that improve its efficiency. First, it is shaped so most of the turning is achieved near mid-chord, reducing viscous losses in the trailing edge region and in the wake. Second, the overall camber is lessened, producing more losses at the leading edge than the original blade, but giving lower overall loss for both compressor and turbine modes.

5.3.2 Effects of Constraints on Optimization

The thickness constraints in the optimization were set based on the geometry of the original double circular arc blade. To determine if there was more to be gained in the design space, each thickness constraint was adjusted and the optimization repeated.[3] The edge thickness was adjusted from 0.6% of chord to 1.0% of chord and Figure 5-11 shows only a small change (~0.001) in RTE as a function of edge thickness. Reducing

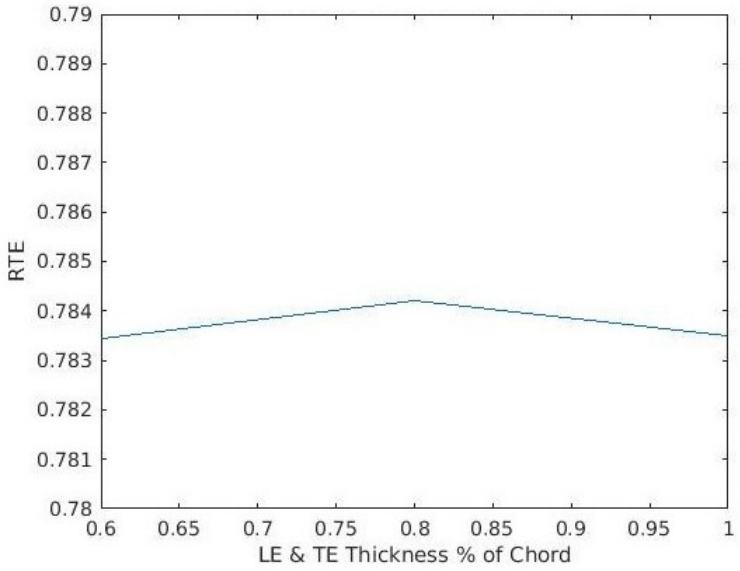

Figure 5-11: RTE For Different Values of Leading and Trailing Edge Thickness

the edge thickness thus does not provide a major benefit in RTE.

We also examine the effect of overall thickness on RTE. The original blade had a maximum thickness of 5.9% of chord and the constraint was varied from 4% to 8%

[3]Optimizations described in this section were carried out using a simple sum of loss coefficients rather than a weighted sum. The weights did not change the optimization results significantly.

of chord, with all other constraints being held as in the original optimization. The RTEs from the resulting blades are shown in Figure 5-12. A smaller overall thickness

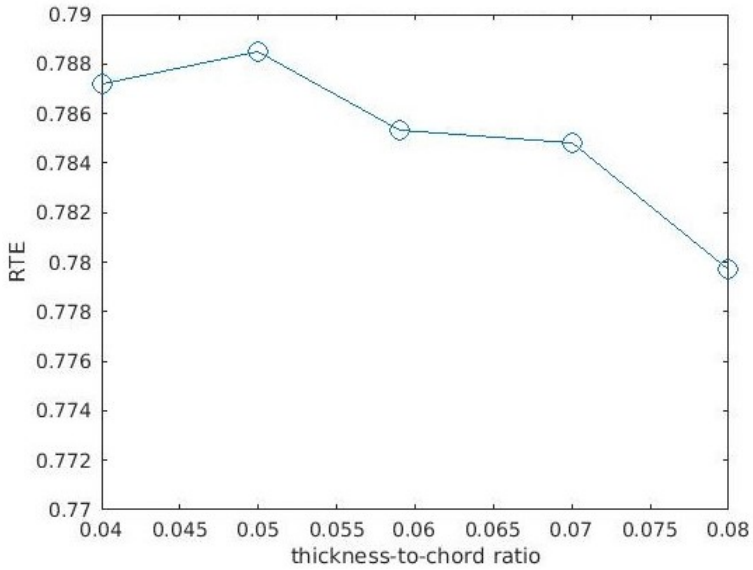

Figure 5-12: RTE For Different Values of Overall Thickness

improves RTE, but the improvement is small compared that attained by optimization.

The effect of solidity was also assessed. Reducing the solidity of a blade row can reduce losses, but it also decreases the flow turning. In this assessment the turning through the passage was held constant, and the blade shape adjusted to compensate. The nominal solidity value from the original double-circular arc is 1, and solidities from 0.8 to 1.1 were examined. Figure 5-13 shows that the RTE is maximized at a solidity of 0.9, with an increase of 0.25 percentage points compared to the optimized blade at a solidity of 1.

5.3.3 Context of 2D Optimization in a 3D turbomachine

It is important to remember that these optimization results are based on 2D computations. The results are still applicable to the blade cross-sections of a 3D turbomachine, and the RTE improvement from optimization will still be present in actual blading, although the values may differ. The loss coefficients, stage efficiencies, and round-trip efficiencies can thus indicate larger increases than a real blade. As discussed in Sec-

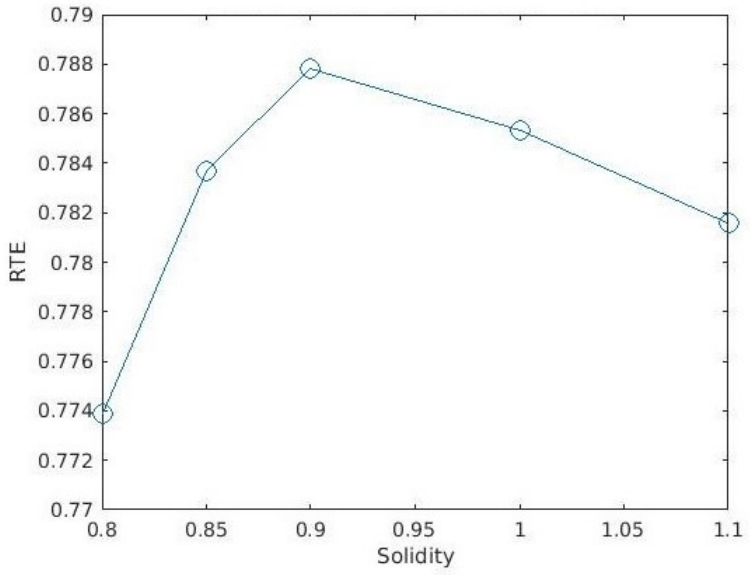

Figure 5-13: RTE For Different Values of Solidity

tion 2.2 however, RTE becomes more sensitive to individual turbomachine efficiency, as the turbomachine efficiency level decreases. Thus, the 2.0 percentage point improvement in RTE could also be an underestimate, as a given loss reduction improves RTE more at lower efficiencies than at higher efficiencies. The primary learning from this Chapter is the guidelines for optimal bi-directional blade shapes, but a full 3D analysis is needed to accurately determine the impact profile optimization has on a real bi-directional turbomachine.

Chapter 6

Summary & Conclusions

6.1 Primary Learnings

The primary learnings in this thesis can be placed into two categories; identifying the requirements of a bi-directional turbomachine and determining best design practices for such a turbomachine. The requirements are those of non-symmetric aerodynamic loading and the need for non-repeating stages. For a pumped thermal energy storage (PTES) system, the aerodynamic loading requirements on the cold turbomachine are such that it does more work as a compressor than as a turbine. Given a fixed blade geometry, this requires different incidence angles in each direction, preventing the turbomachine from operating at maximum efficiency in both directions, and it is the round-trip efficiency (RTE) which is the overall metric that should be maximized. The less-than-maximum turbomachine efficiencies are reflected in the form of an 'RTE penalty' which a conventional PTES system with single-direction turbomachines does not have. The hot turbomachine however, does the same amount of work in both directions, and it can operate closer to maximum efficiency in both directions compared to the cold turbomachine.

The other requirement is the need for non-repeating stages. There is a different amount of work in each direction for the cold machine, and thus different density changes through the turbomachine. As a result, a constant axial velocity cannot occur in both directions. In this thesis, the approach taken is to impose repeating stages

for compressor operation because the compressors were more sensitive to changes in incidence than turbines were.

The design features for a bi-directional turbomachine are described in three parts; number of stages, meanline velocity triangles, and 2D blade profile.

- For a given pressure ratio, a higher stage count results in lower relative blade Mach numbers, reducing the minimum loss and allowing the non-symmetric incidence angles to be closer to those of maximum efficiency. For example, for a heat engine pressure ratio of 3, with counter-rotating turbomachines employed, at least 11 rotors should be used.

- For the double-circular arc blading assessed, the highest RTE was produced with a blade having 33 degrees of camber and with 42 degrees of stagger. The RTE was found to be more sensitive to changes in stage count than changes in camber.

- The 2D efficiency can be improved by shaping the blades such that most turning is done at mid-chord. Additionally, reducing camber while increasing compressor incidence, allowed the turbine to use a less negative incidence. These two actions reduce losses in the trailing edge region of the suction surface in both directions and on the pressure surface in turbine mode. The optimization resulted in an increase in RTE of 2.0 percentage points.

6.2 Future Work

There are several related areas which would be useful to pursue. The first, is to develop best practices that account for three-dimensionality. The 2D calculations suggest the design space provides significant opportunity to advance the technology, and there is some evidence that this will also be true for 3D, but the quantitative benefits need to be addressed.

Another area for future work is the non-repeating stage requirement. In the present work, the decision was made to have repeating stages for operation as a com-

pressor, on the basis that a turbine tends to be more forgiving to variations in incidence. The blade heights could have been scheduled, however, with the turbine using repeating stages and the compressor having different incidence angles for each stage, or for a situation in-between. Further work could assess the impacts of non-repeating stages in each direction including determining the best blade height scheduling for a bi-directional turbomachine.

Finally, the system architecture examined was a counter-rotating turbomachine, so variable stators were not considered as an option to address the non-symmetric flow requirement. It would be useful to examine non-counter-rotating turbomachines, which could use variable vanes and determine the overall trade-offs between the potential for higher efficiencies and the higher number of stages, or larger radius, that would be needed.

THIS PAGE INTENTIONALLY LEFT BLANK

Appendix A

Non-Repeating Stage Calculations

The use of a bi-directional turbomachine means that at least one mode of operation employs non-repeating stages. This appendix details the method in which this requirement is addressed and incorporated into the cycle model.

The blade heights are set so that the turbomachine operates with repeating stages in compressor mode. The turbine stage axial velocity thus varies through the turbomachine, depending on the density change and the set blade heights. To illustrate the physical situation, consider a single compressor blade row where station 1 and 2 are upstream and downstream of the blades, respectively. From continuity, the blade heights for repeating stages are set as in Equation A.1.

$$\frac{H_2}{H_1} = \frac{\rho_1}{\rho_2} \tag{A.1}$$

Using the ideal gas law and the definition of polytropic compressor efficiency,

$$\frac{\rho_1}{\rho_2} = \left(\frac{T_2}{T_1}\right)\left(\frac{P_1}{P_2}\right) = \left(\frac{T_2}{T_1}\right)^{1-\frac{\eta_c \gamma}{\gamma-1}} \tag{A.2}$$

The density ratio, and corresponding height ratio, can also be expressed in terms of the work coefficient.

$$\frac{H_2}{H_1} = \frac{\rho_1}{\rho_2} = \left(1 + Mu_1^2 \psi\left(\gamma - 1\right)\right)^{1-\frac{\eta_c \gamma}{\gamma-1}} \tag{A.3}$$

In Equation A.3, Mu_1 is the corrected speed, as in Equation A.4.

$$Mu_1 = \frac{U}{\sqrt{\gamma R T_{t1}}} \tag{A.4}$$

If the height on either side of the blade row is set, the operation as a turbine is determined, including the ratio between inlet and exit axial velocity.

$$\frac{C_{x1}}{C_{x2}} = \frac{\phi_1}{\phi_2} = \frac{H_1}{H_2}\left(1 + Mu_1^2 \psi\,(\gamma - 1)\right)^{1 - \frac{\gamma}{\eta_t(\gamma-1)}} \tag{A.5}$$

These calculation are carried out for all the turbomachine stages to determine the turbine stage flow coefficients.

Appendix B

Proposed Reconfiguration With Two Heat Rejection Components

In the baseline PTES cycle configuration, the hot machine is symmetric, in that it is designed to achieve the same temperature ratio in both directions. The cold machine is non-symmetric, in that the temperature ratio across the cold machine is different in the two directions forcing it to operate away from peak efficiency, causing a drop in round-trip efficiency. The hot machine on the other hand can operate close to peak efficiency in both directions. It was proposed to reconfigure the PTES cycle such that the pressure ratio is the same in both directions and both machines share the non-symmetry. Although the reconfiguration succeeds in raising the cold turbomachine efficiencies, the changes to the cycle result in a lower round-trip efficiency. This Appendix details the proposed reconfiguration, and why it was not successful in raising RTE.

The concept proposed here splits the heat rejection stage into two parts, so both the charge and generation cycles have the same pressure ratio. The configuration is one heat rejection stage in the same position as the baseline, between the cold storage and recuperator on the generation cycle. and a second heat rejection stage located between the hot storage and the recuperator on the charge cycle. There is thus a non-symmetry across the hot machine and a lesser non-symmetry across the cold machine. A T-S diagram of the proposed configuration is shown in Figure B-1,

overlaid with the original configuration. The heat rejection stages are highlighted.

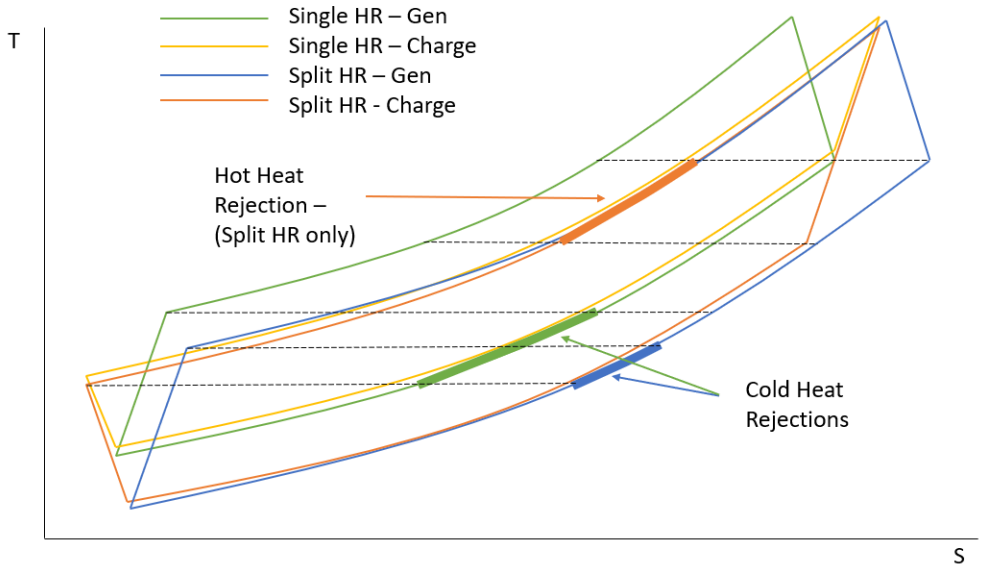

Figure B-1: T-S Diagram of Proposed Split Heat Rejection Configuration

With the proposed configuration, both the hot and cold machines operate away from their peak efficiency. The drop in round-trip efficiency that comes from the turbomachines being operated away from peak efficiency however, is smaller than with the baseline configuration, as in Figure B-2, which shows the efficiency curves of an example geometry as both compressor and turbine. Four sets of points are marked on the curves. These are the incidence angles at which round-trip efficiency is maximized for the hot and cold machines of each configuration. The difference between these incidence angles directly correlates with the amount of non-symmetry across the turbomachine.

Figure B-2 illustrates that the incidence angles of the cold machine move closer together with the proposed configuration, and that the hot machine incidences angles move apart in the new configuration. As these incidence angles move, the turbomachine efficiencies can be closer to maximum.

Despite the apparent advantage of a configuration with split heat rejection, the round-trip efficiency is actually lower for this alternate setup. To explain why, the definition of round-trip efficiency needs to be revisited. For this explanation, the most

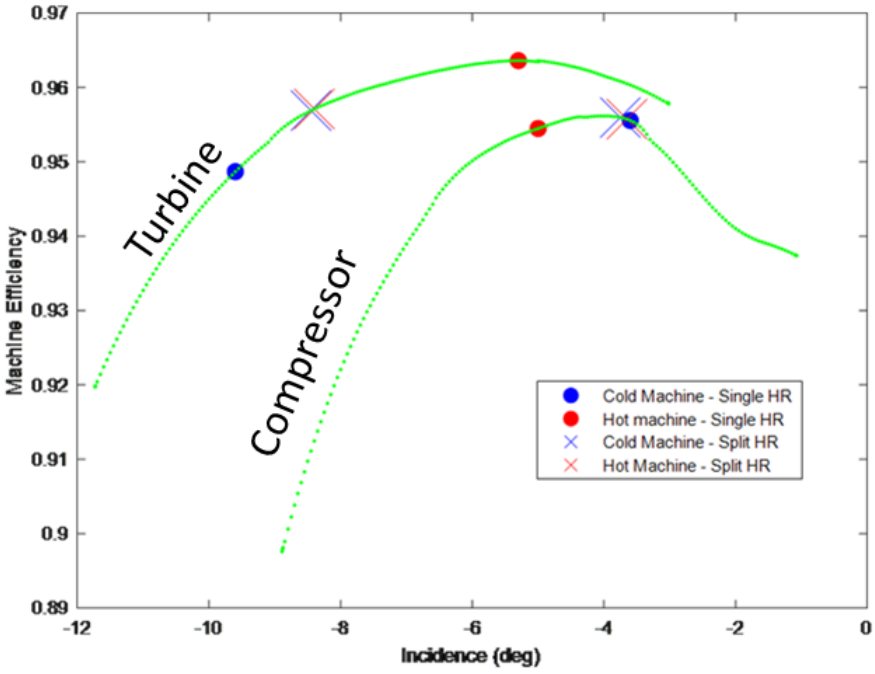

Figure B-2: Efficiency Curves and Incidence Angles of Maximum RTE

convenient definition of RTE is the product of the heat engine's thermal efficiency and the heat pump's coefficient of performance. When viewed in this regard, the major differences between the two configurations (single and split heat rejection) can be seen. To give an unobscured comparison, the two configurations are simulated with constant values of turbomachine efficiency. Figure B-3 show how the Brayton efficiency and COP react to a change in turbomachine efficiency for each setup.

The heat pump COP is lower with a split heat rejection setup than with the baseline single heat rejection setup. The efficiency of the heat engine is higher with the split heat rejection setup. Unfortunately, these two effects do not balance and the round-trip efficiency is lower for the proposed configuration. Figure B-4 shows how RTE changes with turbomachine efficiency for each configuration.

In summary, the proposed configuration introduces a second heat rejection stage, allowing both charge and generation cycles to operate with the same pressure ratio. This configuration succeeds in sharing the temperature ratio non-symmetry between both the cold machine and the hot machine, leading to higher turbomachine efficien-

cies. The changes to the charge and generation cycles however, leads to an inherently lower round-trip efficiency for the proposed configuration, despite the higher turbomachine efficiencies.

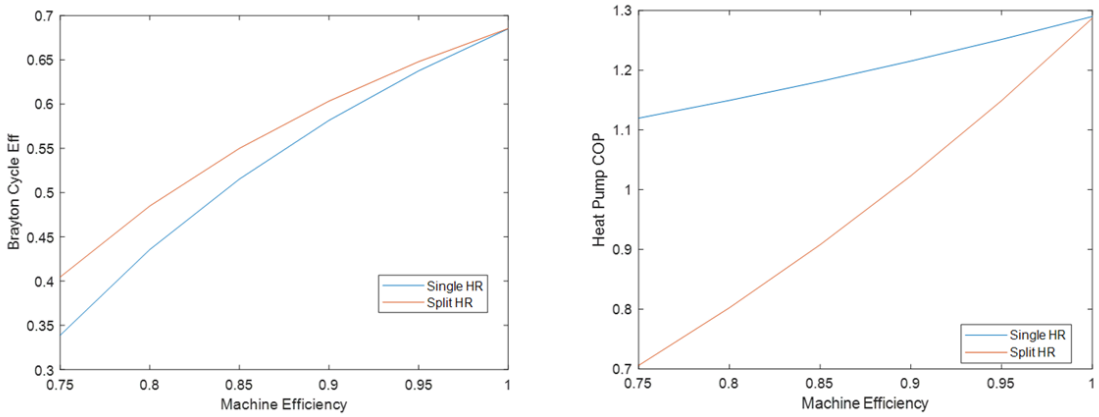

Figure B-3: Heat Engine Brayton Efficiency and Heat Pump COP for each Configuration

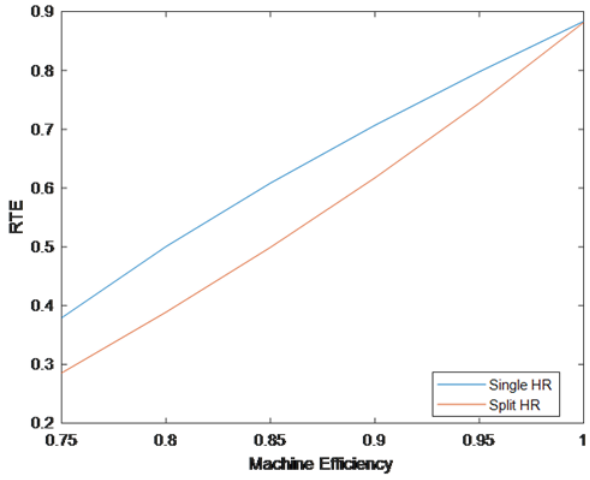

Figure B-4: RTE vs. Turbomachine Efficiency for each Configuration

Appendix C

Proposed Reconfiguration With Three Turbomachines

As discussed in Section 3.1, the PTES cycle places non-symmetric loading requirements on the cold turbomachine. Figures 3-1 and 3-2 show how this requirement forces the cold machine to operate away from its maximum efficiency in both directions, resulting in an RTE penalty. The hot turbomachine however, does not have the same requirement. It does the same amount of work in both directions, operating between points 4 and 5 on the T-S diagram in Figure 2-2. Therefore, it can operate much closer to its own maximum efficiency in both directions. Figure C-1 shows the same efficiency vs. incidence angle curves as Figure 3-1, but for the hot machine.

In Figure C-1, the green circles, indicating the pair of hot machine incidence angles for which RTE is maximized, are closer together than they are for the cold machine. This allows the hot machine to operate near its maximum efficiency in both directions, unlike the cold machine. Analogous to the cold machine discussion in Section 3.1, Figure C-2 shows the RTE penalty from to the hot machine alone, which is much smaller than the cold machine.

With the different properties of the hot and cold machines in mind, there may be an opportunity to minimize the overall RTE penalty compared to a conventional PTES system. The concept is to use 3 turbomachines; 1 bi-directional hot machine, and 2 single-direction cold machines. Using 3 turbomachines would eliminate the

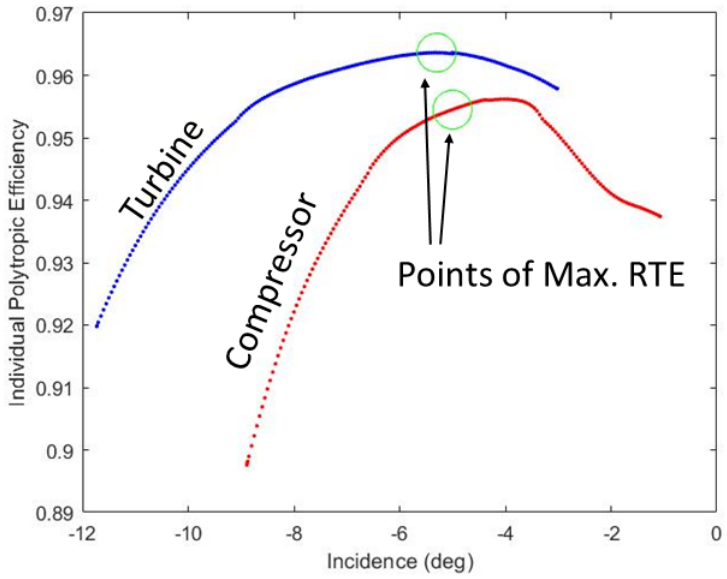

Figure C-1: Hot Machine Compressor and Turbine Individual Efficiency vs. Incidence

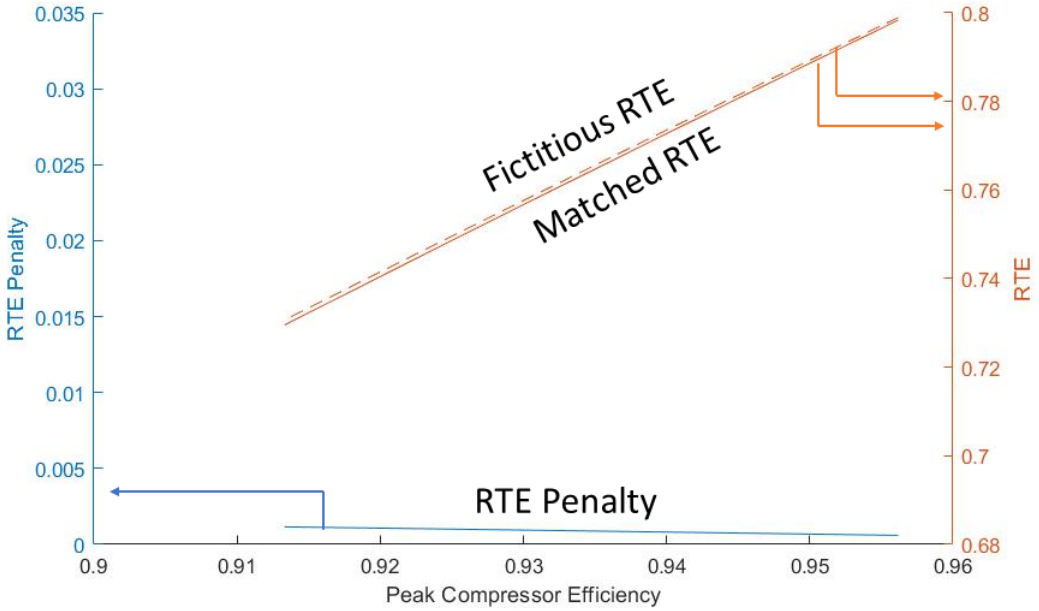

Figure C-2: RTE Penalty from Hot Machine

RTE penalty associated with the bi-directional cold machine, bringing the RTE close to that of a conventional PTES system, while saving some cost and complexity by using only 1 hot machine. The decision of what PTES configuration is best is based on a trade-off between cost and round-trip efficiency, and is beyond the scope of this thesis. Aerodynamically however, the bi-directional cold machine has the largest impact on RTE, which a 3 turbomachine setup would eliminate.

THIS PAGE INTENTIONALLY LEFT BLANK

Bibliography

[1] Nicholas A. Cumpsty. *Compressor Aerodynamics*. Longman Scientific & Technical, 1989.

[2] Paul Denholm, Erik Ela, Brendan Kirby, and Michael Milligan. The role of energy storage with renewable electricity generation. Technical report, National Renewable Energy Laboratory, 2010.

[3] Tony Dickens and Ivor Day. The design of highly loaded axial compressors. In *Proceedings of ASME Turbo Expo 2009: Power for Land, Sea and Air*, 2009.

[4] S. L. Dixon and C. A. Hall. *Fluid Mechanics and Thermodynamics of Turbomachinery - 6th Ed.* Elsevier, 2010.

[5] Mark Drela. *A User's Guide to LINDOP V2.50*. MIT Department of Aeronautics and Astronautics, Cambridge, MA, June 1996.

[6] Mark Drela. *Flight Vehicle Aerodynamics*. The MIT Press, 2014.

[7] Mark Drela and Harold Youngren. *A User's Guide to MISES 2.63*. MIT Aerospace Computational Design Laboratory, Cambridge, MA, February 2008.

[8] David K. Hall. Performance limits of axial turbomachine stages. Master's thesis, Massachusetts Institute of Technology, 2011.

[9] James Kesseli. Reversible counter-rotating turbomachine to enable brayton-laughlin cycle. Technical report, U. S. Department of Energy, 2018.

[10] James Kesseli. Reversible turbomachine to enable laughlin brayton cycle for thermally pumped electrical energy storage: Quarter 1. DAYS Technical Review, June 2019.

[11] James Kesseli. Reversible turbomachine to enable laughlin brayton cycle for thermally pumped electrical energy storage: Quarter 5. DAYS Technical Review, May 2020.

[12] Robert B. Laughlin. Pumped thermal grid storage with heat exchange. *Journal of Renewable and Sustainable Energy*, 2017.

[13] J. J. Waldren, C. J. Clark, S. D. Grimshaw, and G. Pullan. Non-dimensional parameters for comparing conventional and counter-rotating turbomachines. In *Proceedings of ASME Turbo Expo 2019: Turbomachinery Technical Conference and Exposition*, 2019.